

HELEN DORRINGTON – MASTER’S THESIS – MCMASTER UNIVERSITY

SYNTHESIS AND CHARACTERIZATION OF IN SITU GELLING HYDROGELS MADE  
FROM HYPERBRANCHED POLY(OLIGOETHYLENE GLYCOL METHACRYLATE)

By HELEN DORRINGTON, B.Eng & Biosciences

A Thesis Submitted to the School of Graduate Studies in Partial Fulfilment of the Requirements  
for the Degree Master of Applied Science

McMaster University © Copyright by Helen Dorrington, August 2016

MASTER OF APPLIED SCIENCE (2016)

Department of Chemical Engineering

McMaster University

Hamilton, Ontario

TITLE: Synthesis and Characterization of In Situ Gelling Hydrogels Made From Hyperbranched Poly(oligoethylene glycol methacrylate)

AUTHOR: Helen Dorrington, B. Eng & Biosciences (McMaster University)

SUPERVISOR: Dr. Todd Hoare

NUMBER OF PAGES: xiii, 90

## ABSTRACT

Hydrogels have attracted interest as biomaterials due to their similarity to native tissue and extracellular matrix as well as their versatility and tunability. Each of these characteristics allows hydrogels to be used in a wide variety of biomedical applications including drug delivery, tissue engineering, and regenerative medicine. Poly(oligoethylene glycol methacrylate) (POEGMA) has been shown to possess attractive biological and thermoresponsive properties, serving as an alternative to both poly(ethylene glycol) (PEG) and poly(N-isopropylacrylamide) (PNIPAM) depending on the number of ethylene oxide repeat units in the POEGMA side chain. Our group has shown the versatility of POEGMA and has successfully developed hydrazide- and aldehyde-functionalized polymer precursors that form an injectable *in situ* gelling hydrogel. By engineering the precursor polymer structure and crosslinking density (i.e. number of reactive functional groups in the precursor polymers), the properties of these hydrogels can be tuned. Herein, a hyperbranched structure was incorporated into POEGMA precursors to control the physical and biological properties of hydrogels independent of the chemistry while maintaining gel injectability. By varying the degree of branching (DoB) in these precursors, it was possible to tune the hydrogel properties based on reacting combinations of hyperbranched-linear and hyperbranched-hyperbranched precursor polymers. While it was feasible to tune the mechanical properties of the hyperbranched hydrogels based on the DoB, the hyperbranched-hyperbranched system showed diminished mechanical strength when compared to the hyperbranched-linear system. Overall, the mechanical properties of the whole hydrogel series were comparable

to previously reported linear POEGMA hydrogels. In terms of swelling and degradation kinetics, the swelling and degradation rate in both acid-catalyzed conditions and in phosphate-buffered saline (PBS) at physiological temperature (37°C) correlated with DoB and polymer size. The precursor polymers showed minimal cytotoxicity in the presence of 3T3 mouse fibroblasts. Lastly, each of the hyperbranched hydrogels adsorbed higher quantities of protein compared to PEG-based hydrogels, but still relatively low amounts compared to other polymeric biomaterials. We have shown that it is possible to significantly tune the physicochemical properties by slightly changing the polymer precursor chemistry, namely by varying the amount of crosslinker and, thus, the degree of branching in the polymer network. Therefore, hyperbranched POEGMA offers a versatile platform to create tunable hydrogels based on polymer precursor structure for biomedical applications.

## ACKNOWLEDGEMENTS

There are many people to whom I owe my utmost gratitude for their help, guidance, and love throughout my time at McMaster University. First and foremost, I would like to thank my supervisor, Dr. Todd Hoare. It has been a pleasure to work in his lab for the last five years, both as a summer student and as a graduate student. His encouragement and guidance is greatly appreciated. I have been given so many opportunities to expand my academic and research horizons that I would not have had otherwise. These experiences will stay with me throughout my engineering career.

I must also thank everyone in the Hoare lab for their dedication to science and for their friendship. Special thanks goes to Niels Smeets and Emilia Bakaic for taking me under their wing and showing me all the wonderful ways of POEGMA. Without your mentoring and wisdom, I most definitely would not be at this point today. I also appreciate all the help and guidance from Ivan Urosev, my amazing partner in science for this thesis project, as well as Donovan Ramkishun. The content of this paper is a testament to all of *our* hard work. I look forward to many more celebratory “meetings” at The Phoenix.

Lastly, I would like to wholeheartedly thank my friends and family for being a spectacular support network throughout my undergraduate and graduate programs. To my parents, Joe and Elizabeth, I cannot express how much I appreciate everything you have done for me in the past 24 years. I will always remember to “stay together, hold hands, and remember where I came from”. To the best friends anyone could ask for – Shelby Olesovsky, Nicole Mangiacotte, Robin Ng, and the rest of my Chem Bio crew – thank you for putting up with me for all these years. I literally would have gone insane without you. Last, but certainly not least, thank you to my boyfriend, Owen Hempel. I cherish the encouragement, love, and support you’ve given me throughout this past year. I look forward to many more good times with all of you.

## TABLE OF CONTENTS

<b>1. Introduction</b>	<b>1</b>
1.1. Hydrogel Fundamentals	3
1.2. Poly(oligoethylene glycol methacrylate)	8
1.3. Hyperbranched Polymers	12
1.4. Hyperbranched Polymer Assemblies and Hydrogels	25
<b>2. Hydrogels Prepared with Hyperbranched Building Blocks</b>	<b>30</b>
2.1. Introduction	30
2.2. Materials and Methods	35
2.2.1. Materials	35
2.2.2. Polymer Synthesis	37
2.2.3. Hydrazide Functionalization	38
2.2.4. Aldehyde Functionalization	38
2.2.5. Polymer Characterization	39
2.2.6. Preparation of Hydrogels	42
2.2.7. Residual Functional Groups Labelling	42
2.2.8. Hydrogel Rheology	43
2.2.9. Hydrogel Transparency	43
2.2.10. Swelling and Degradation Kinetics	44
2.2.11. Cytotoxicity	45
2.2.12. Protein Adsorption	45
2.3. Results and Discussion	46
2.3.1. Polymer Characterization	46
2.3.2. Hydrogel Rheology	54
2.3.3. Swelling and Degradation Kinetics	59
2.3.4. Cytotoxicity of Polymer Precursors	65
2.3.5. Protein Adsorption	66
<b>3. Conclusions and Future Directions</b>	<b>69</b>
<b>4. References</b>	<b>73</b>
<b>5. Appendix – Supplementary Information</b>	<b>81</b>

## LIST OF FIGURES

- Figure 1.1.** 11  
Typical synthesis of POEGMA polymer precursors and hydrogels using hydrazone chemistry. Image adapted from the literature (Smeets, Bakaic, et al. 2014).
- Figure 1.2.** 13  
Schematic of various branched polymer architectures – (a) star, (b) brush or comb, (c) “pom-pom”, (d) dendigraft, (e) hyperbranched, and (f) dendrimer. Image adapted from the literature (England, et al. 2010).
- Figure 1.3.** 23  
General mechanism of reversible addition-fragmentation chain transfer (RAFT) polymerization.
- Figure 1.4.** 28  
Scheme of hyperbranched polymer synthesis using RAFT. For this project, the “monomers” were OEGMA and MAA, the “brancher” was EGDMA, the initiator was AIBN, and “RSH” or the RAFT agent was CPCBD. Image adapted from the literature (Voit, et al. 2009).
- Figure 2.1.** 41  
 $^1\text{H-NMR}$  spectra for  $\text{HBP}_{\text{H}1522}$  (A) and  $\text{HBP}_{\text{A}0}$  (B) hyperbranched POEGMA polymers in  $\text{DMSO-d}_6$ . Note that since  $\text{HBP}_{\text{A}0}$  is a linear polymer prepared without crosslinker – there are no EGDMA or pendant groups present (i.e. side chains w and z in the chemical structure are not represented in the spectrum).
- Figure 2.2.** 48  
Scheme for the hypothesized growth mechanism of the hyperbranched polymer precursors. The top image shows growth for less branched molecules, while the bottom depicts growth for more highly branched molecules.
- Figure 2.3.** 54  
Measurements of relative fluorescence of hydrazide-reactive FITC bound to unreacted hydrazide functional groups in all hyperbranched-linear and hyperbranched-hyperbranched POEGMA hydrogels. Error bars for each measurement represents one standard deviation value from the mean ( $n = 4$ ).

- Figure 2.4.** 55  
Mechanical properties of the varying DoB series of hyperbranched POEGMA hydrogels at 22°C. Error bars for each measurement represents one standard deviation value from the mean ( $n = 3$ ).
- Figure 2.5.** 57  
Mechanical properties of the 15% DoB hyperbranched POEGMA hydrogel series at 22°C. Error bars for each measurement represents one standard deviation value from the mean ( $n = 3$ ).
- Figure 2.6.** 61  
Degradation kinetics of the varying DoB series of hyperbranched POEGMA hydrogels in 10 mM HCl at 37°C. Error bars for each measurement represents one standard deviation value from the mean ( $n = 3$ ).
- Figure 2.7.** 62  
Degradation kinetics of the 15% DoB hyperbranched POEGMA hydrogel series in 10mM HCl at 37°C. Error bars for each measurement represents one standard deviation value from the mean ( $n = 3$ ).
- Figure 2.8.** 64  
Swelling kinetics of the varying DoB series of hyperbranched POEGMA hydrogels in 10mM PBS at 37°C. Error bars for each measurement represents one standard deviation value from the mean ( $n = 3$ ).
- Figure 2.9.** 65  
Swelling kinetics of the 15% DoB hyperbranched POEGMA hydrogel series in 10mM PBS at 37°C. Error bars for each measurement represents one standard deviation value from the mean ( $n = 3$ ).
- Figure 2.10.** 66  
Relative viability of 3T3 mouse fibroblasts treated with each polymer for 24 hours at concentrations ranging from 0.2 to 2 mg/mL. Error bars for each measurement represents one standard deviation value from the mean of measured percent cell viability ( $n = 4$ ).

<b>Figure 2.11.</b>	68
Adsorption of BSA to hyperbranched POEGMA hydrogels. Error bars for each measurement represents one standard deviation value from the mean ( $n = 4$ ).	
<b>Figure S.1.</b>	81
SEC chromatogram of HBP <sub>H</sub> 15 <sub>22</sub> with collected samples during polymerization reaction.	
<b>Figure S.2.</b>	82
SEC chromatogram of HBP <sub>H</sub> 15 <sub>25</sub> with collected samples during polymerization reaction.	
<b>Figure S.3.</b>	83
SEC chromatogram of HBP <sub>H</sub> 10 with collected samples during polymerization reaction.	
<b>Figure S.4.</b>	84
SEC chromatogram of HBP <sub>H</sub> 5 with collected samples during polymerization reaction.	
<b>Figure S.5.</b>	85
SEC chromatogram of HBP <sub>H</sub> 0 with collected samples during polymerization reaction.	
<b>Figure S.6.</b>	86
SEC chromatogram of HBP <sub>A</sub> 15 with sample taken at the end of polymerization.	
<b>Figure S.7.</b>	87
SEC chromatogram of HBP <sub>A</sub> 0 with sample taken at the end of polymerization.	
<b>Figure S.8.</b>	88
Molecular weight, conversion, and polydispersity kinetics during the 9 hour polymerization reaction at 70°C. Samples were taken at 0, 2, 4, 6, and 9 hours.	
<b>Figure S.9.</b>	89
Swelling kinetics of the varying DoB series of hyperbranched POEGMA hydrogels in 10mM PBS at 22°C. Error bars for each measurement represents one standard deviation value from the mean ( $n = 3$ ).	
<b>Figure S.10.</b>	90
Swelling kinetics of the 15% DoB hyperbranched POEGMA hydrogel series in 10mM PBS at 22°C. Error bars for each measurement represents one standard deviation value from the mean ( $n = 3$ ).	

## LIST OF TABLES

<b>Table 2.1.</b>	37
Synthesis of hyperbranched POEGMA polymer series.	
<b>Table 2.2.</b>	51
Chemical characteristics of the synthesized hyperbranched and linear POEGMA polymers. All polymers were polymerized for 9 hours except for the HBP <sub>H</sub> 15 <sub>25</sub> polymer, which was polymerized for 10.5 hours. Composition, functionalization, and DoB values were calculated using NMR and titration data. Molecular weight and PDI values were obtained from aqueous SEC. Cloud point values were > 90°C for all polymers and were determined using UV-vis spectrophotometry.	
<b>Table 2.3.</b>	52
Comparison of gelation time for various hyperbranched-linear and hyperbranched-hyperbranched polymer combinations at 22°C (20 wt% of each reactive polymer).	
<b>Table 2.4.</b>	59
Comparison of shear storage modulus, compressive modulus, and transmittance (at 595 nm) for each hyperbranched hydrogel at 22°C. For reference, the same volume of PBS has an average transmittance of 92.0% at 22°C in the measurement plate. Error values for each measurement represents one standard deviation value from the mean ( $n = 3$ ).	

## LIST OF ABBREVIATIONS

ADA	Aminoacetaldehyde diethyl acetal
ADH	Adipic acid dihydrazide
AIBN	Azobisisobutyronitrile
BSA	Bovine serum albumin
CPCBD	2-cyano-2-propyl-4-cyanobenzodithioate
DoB	Degree of branching
DCM	Dichloromethane
DI	Milli-Q grade distilled deionized water
DLS	Dynamic light scattering
DMEM	Dulbecco's modified Eagle medium (high glucose, high pyruvate)
DMSO-d <sub>6</sub>	Deuterated dimethyl sulfoxide
ECM	Extracellular matrix
EDC	N'-ethyl-N-(3-dimethylaminopropyl)-carbodiimide
EGDMA	Ethylene glycol dimethacrylate
FITC	5-Fluorescein isothiocyanate
FTSC	Fluorescein-5-thiosemicarbazide
HBP <sub>H/A</sub> #	Hyperbranched POEGMA polymer – subscript: functional group (H – hydrazide; A – aldehyde); number: targeted DoB percentage

HBX <sub>y</sub>	Hyperbranched POEGMA hydrogel – X: targeted DoB percentage of precursors; y: modifications to one or both of the polymer precursors
HCl	Hydrochloric acid
LCST	Lower critical solution temperature
MAA	Methacrylic acid
MW	Molecular weight
NaOH	Sodium hydroxide
NHS	N-Hydroxysuccinimide
NMR	Nuclear magnetic resonance spectroscopy
OEGMA	Oligo(ethylene glycol) methacrylate
PBS	Phosphate-buffered saline
PDI	Polydispersity
PEG	Polyethylene glycol
PNIPAM	Poly(N-isopropylacrylamide)
POEGMA	Poly(OEGMA)
PS	Penicillin streptomycin
RAFT	Reversible addition-fragmentation chain transfer
SEC	Size exclusion chromatography
VPTT	Volume phase transition temperature
3T3	<i>Mus musculus</i> mouse fibroblast cells

## **DECLARATION OF ACADEMIC ACHIEVEMENT**

The work presented in this thesis was completed by the author, with the guidance and consultation of Dr. Todd Hoare, except for the following contributions:

Chapter 2: Ivan Urosev assisted in the design, synthesis, and characterization of all hyperbranched polymers, which are listed in Tables 2.1 and 2.2 as well as Figure S.8. Donovan Ramkishun performed some of the swelling and degradation assays, the data for which went into the creation of Figures 2.7, 2.9, and S.10.

## **Chapter 1 – Introduction**

Finding a suitable biomaterial to replace and/or supplement damaged or diseased tissue has been a key focus of research for several years. Biomaterials appropriate for such function can be derived from both natural and synthetic materials; however, synthetic scaffolds have been of special interest based on their more consistent, robust, and highly tunable nature (Place et al., 2009). Biomaterials can be applied in a multitude of applications, each with their own needs. Therefore, it is difficult to produce a material that would fit a “one size fits all” profile. Furthermore, it would be advantageous to create a biomaterial that can be adapted to suit the requirements of the patient and their affliction for a more customized therapy. Either way, a successful biomaterial must be able to aid in the regeneration of tissue and/or the restoration of a non-diseased state and function in the appropriate manner in the targeted area while exhibiting an appropriate host response based on the application for which it is being used (Williams, 2008).

Hydrogels are interesting materials that have been widely studied for use in a variety of applications including tissue engineering and regenerative medicine, wound healing, and drug delivery, among others (Gaharwar et al., 2014). These water-swollen polymer networks are able to mimic native extracellular matrix and are therefore seen as an attractive biomaterial for use *in vivo*. Furthermore, hydrogel properties are highly controllable and tunable, making it possible to create polymers that closely mimic a vast array of soft tissues and use them in the replacement and supplementation in such areas (Van Tomme et al., 2008). Based on the rational engineering of gel precursor materials

and the utilization of various crosslinking chemistries, modular design of hydrogel-based biomaterials is achievable.

While a variety of polymers have been used to create hydrogels for use in biomedical applications, our group has shown that poly(oligoethylene glycol methacrylate) (POEGMA) is an attractive alternative to both polyethylene glycol (PEG) and poly(N-isopropylacrylamide) (PNIPAM) for various reasons that will be discussed in the following sections. Based on the length of the ethylene glycol side chain in the monomer incorporated into the polymer precursor, it is possible to synthesize a functionalizable POEGMA polymer that is non-cytotoxic, non-biofouling, and thermoresponsive (Lutz, Akdemir et al., 2006). The free radical polymerization mechanism for these materials allows for easy control over molecular weight via a range of controlled radical chemistries as well as modification and functionalization via simple copolymerization. Furthermore, with the use of hydrazone chemistry for making such gels as pioneered in our group, these POEGMA polymer precursors can be used to form injectable *in situ* gelling hydrogels, making them excellent biomaterial candidates.

The work discussed in this thesis describes how hydrogels synthesized from POEGMA precursors are able to overcome some of the common limitations of typical biomaterials. While linear polymer structures are frequently used in the literature, other, more complex structures offer enhanced chemical and physical property variations for improved modular design. In this view, a series of hyperbranched POEGMA hydrogels was created to show the tunability of such materials and how the branched structure of hydrogel precursors affects hydrogel properties. The subsequent literature review will

outline the current relevant research background of this work. An in depth exploration of hyperbranched polymers will then summarize what these macromolecules are, how they are synthesized, and what benefits they have to offer in terms of advances in biomedical engineering. For the basis of this project, this synopsis will also introduce the comparison between hyperbranched and linear polymers as well as combinations thereof. Effects of the hyperbranched polymer structure, in terms of variations in the degree of branching, will be especially highlighted. Chapter 2 will outline and explain how this thesis addressed the current limitations and challenges faced in the realm of hydrogel-based biomaterials. The results from this work will attempt to show how variations in POEGMA polymer architecture can affect the overall physical and chemical hydrogel characteristics in the hopes of attaining injectable, *in situ*-gelling hydrogels with more desirable properties.

### **1.1. Hydrogel Fundamentals**

Hydrogels are water-swollen polymeric networks that can be composed of natural or synthetic materials. Since these materials are generally soft, flexible, and possess a high water content, they appear to closely mimic native tissue or extracellular matrix (Aziz et al., 2015). These attributes make hydrogels a prime candidate for a biomaterial with applications in tissue engineering, regenerative medicine, drug delivery, diagnostics, cellular immobilization, etc. (Gaharwar et al., 2014; Hoare et al., 2008; Wu et al., 2008; Khademhosseini et al., 2007). However, while great strides have been made in this area of research, limitations remain in terms of achieving hydrogels that fit all the design criteria of biomaterial use in a clinical setting. Specifically, both hydrogels and their polymer

precursors must be highly reproducible, manufacturable, approvable from a regulatory perspective, and affordable for both physicians and patients. Furthermore, extensive testing for safety and efficacy must be performed. This may involve both *in vitro* and *in vivo* models as well as a variety of assays for cytotoxicity, mutagenesis and carcinogenesis, and inflammation. The results from such analyses may provide insight as to how the biomaterial may interact with the host (i.e. patient) upon implantation (Aziz et al., 2015). Along these lines, a select few polymers including hyaluron (HA)- and PEG-based materials have shown to be useful for *in vitro* and *in vivo* applications, indicating potential use for further study (Prestwich, 2007).

Overall hydrogel properties are dependent on the properties of the polymer precursors as well as how they are assembled to form a hydrogel network. Such interactions could be of either a chemical or physical nature, based on the polymer composition and crosslink density, and affect properties such as mechanical strength and drug release kinetics (Mateen et al., 2014). Examples of physical crosslinking include hydrophobic interactions (Xiong et al., 2006), charge interactions (Chen, 2005), hydrogen bonding (Gupta et al., 2006), stereocomplexation (Tsuji, 2005), and supramolecular chemistry (Li et al., 1994). Each of these has their own advantages and disadvantages. Hydrophobic interactions within a polymer network often give rise to “sol-gel” transitions - aqueous solutions that, once triggered, form a gel. For example, chitosan grafted with poly(ethylene glycol) (PEG) forms a thermoresponsive system, which gels when exposed to a temperature of 37°C (Bhattarai et al., 2005). While many hydrogels are able to respond to external stimuli such as pH, UV light, or enzymatic activity, thermoresponsive

hydrogels are systems that specifically respond to changes in temperature via a sol-gel transition. This is typically defined by the presence of a lower critical solution temperature (LCST) in the polymer precursor, where the polymer will become insoluble above a certain threshold (Bernstein et al., 1977). This transition could be the driving force for gelation or physical changes in the hydrogel network such as swelling upon entering a heated environment (i.e. being injected *in vivo* at physiological temperature). These types of responses can be exploited for applications such as drug delivery and tissue engineering (Klouta et al., 2008). Therefore, hydrophobic interactions may arise as a result of crosslinking or a physical response. On the other hand, charge interactions via ionic interactions between oppositely charged functional groups can also drive gelation, in addition to reversible crosslinking via functional group ionization/protonation when there is a change in pH. An example of such crosslinking is the interaction between anionic and cationic polymer coated dextran microspheres, which gel upon mixing based on the ionic complex that forms between particles (Van Tomme et al., 2005). Hydrogen bonding and stereocomplexation can be exploited in hydrogel formation, but only if the polymer precursors are comprised of functionalities that allow such interactions. Supramolecular chemistry can be used in a similar manner, with self-assembly via specific molecular recognition moieties being the driving force behind the self-assembly of the polymer network (Li et al., 1994).

From a chemical crosslinking perspective, crosslinking may occur via the use of small molecule crosslinkers that mediate crosslinking between polymer chains and/or direct polymer-polymer crosslinking between polymer-incorporated functional groups.

Examples of the use of small molecule crosslinkers include dextran-tyramine crosslinked with horseradish peroxidase and hydrogen peroxide that have been found to make fast-gelling hydrogels (Jin et al., 2007). However, it is also possible that the drug payload within the polymer network may also act as a crosslinker in cases in which the drug contains two available functional groups. Unfortunately, there have been instances of cytotoxicity reported due to residual small molecules (Beena et al., 1995). Alternately, while functionalizing the polymer precursors with reactive functional groups may require significant post-polymerization modification, it is possible to adjust properties, such as gelation time, simply by varying the type of functional group/linkage mechanism or functional group density and the potential issues of reactive small molecule toxicity are largely minimized (Hoare et al., 2008).

Since modifications to these crosslinking techniques are relatively easy, it is possible to control individual hydrogel properties in a facile manner, including crosslinking density, swelling and degradation kinetics, mechanical strength, and release kinetics. For example, if the crosslink density increases, there is typically a higher mechanical strength, lower swelling ratio, and decreased mesh size and diffusion exhibited in the hydrogel (Nicodemus et al., 2008). Furthermore, the ability to tune the polymer precursor properties and composition allows for the modular design of smart materials that can be responsive to external stimuli (Purcell et al., 2014). Of particular interest for *in vivo* applications, Heskins and Gillet originally described a poly(N-isopropylacrylamide) (PNIPAM) system that has a LCST transition around physiological temperature. Therefore, when the PNIPAM hydrogel is subjected to temperatures of 37°C

or higher, the polymer chains collapse and the mesh becomes more hydrophobic (Heskins et al., 1968). By incorporating different functional groups and polymer backbones, it is also possible to synthesize a hydrogel that is responsive to light, pH, enzymatic activity, or other stimuli (Purcell et al., 2014; Wu et al., 2008).

The creation of a hydrogel that is responsive and adaptive to the local microenvironment in which it is implanted into the body would be ideal for applications in drug delivery and tissue engineering (Rami et al., 2014; Khademhosseini et al., 2007). To be used for this purpose, a hydrogel must meet a variety of requirements in order to be considered an adequate substitute for native tissue or other biomaterial. These include, but are not limited to, possessing a level of porosity that would allow for cell and vascular integration, comprising materials that exhibit controllable biological properties, avoiding any adverse host responses, displaying mechanical properties that closely mimic the native tissue in the area of interest, having a surface chemistry that allows cells to adhere and proliferate, and being easy to produce and form an array of shapes and sizes (Rami et al., 2014). For the specific application of drug delivery, hydrogel systems must have a porosity that is controllable, but allows for the diffusion release of the target payload(s) while still maintaining a high drug concentration locally at the implantation site to ensure drug delivery is relevant over a prolonged period. However, in many cases there is a burst release observed within the first few hours to days caused by the inherently high water content and typically weak interactions between most (hydrophilic) drugs and hydrogels. To minimize or prevent this, the interactions between the hydrogel network and the drug itself must be enhanced to slow drug diffusion. A number of methods have been

employed for this purpose, including the introduction of physical interactions such as charge, covalent linkages between the drug and the hydrogel enabling control over the release rate by the rate of bond cleavage, or increased crosslinks or structural complexity (Purcell et al., 2014; Hoare et al., 2008).

Despite the many advantages of hydrogels and their use in biomedical applications, there are still an assortment of challenges and limitations that these materials must overcome. Importantly, hydrogel systems must be tunable, with controllable properties, and be easy to administer in a clinical setting. Even with a growing interest in this field, creating a hydrogel material with optimized physicochemical properties while avoiding off-target effects and invasive surgical implantation is proving to be fairly difficult. The key will be to be able to synthesize a material that is compatible with the body (including degradation products), comprises a structure and chemistry that is easily modified and tuned for optimized hydrogel properties, and can be administered in a non-invasive manner (i.e. injection).

## **1.2. Poly(oligoethylene glycol methacrylate)**

Finding the right polymer for the synthesis of a hydrogel is pivotal for creating an ideal biomaterial. One of the most widely used polymers in this context is poly(ethylene glycol) or PEG (Bakaic, Hoare et al., 2015; Koehler et al., 2013; Peppas et al., 1999). PEG is one of few polymers that have been approved by the Food and Drug Administration (FDA) for use in biomedical applications. This material's success is mainly attributed to its hydrophilic, non-immunogenic, and non-cytotoxic qualities (Smeets, Bakaic et al., 2014). This polymer resists protein and cellular adhesion,

preventing unwanted host responses and allowing for effective masking of the biomaterial being introduced into the body (Smeets, Patenaude et al., 2014). Based on a vast number of *in vitro* and *in vivo* studies, PEG has proven to be an attractive candidate for use in drug delivery, tissue replacement/supplementation, scaffolds for tissue engineering and cell delivery, and wound dressings (Bakaic, Hoare et al., 2015; Lin et al., 2009). However, there are a number of disadvantages to using PEG, including low mechanical strength (only partially mitigated by using more expensive and complex star morphology polymers), poor drug-hydrogel interactions causing low drug loading and rapid burst release of payload, as well as high swelling ratios. Furthermore, even though PEG can be synthesized via a relatively simple ring-opening process, the only functional groups available for further modification are at the chain ends. Since any functional modification and crosslinking must then occur using these functional groups, adding functionality essentially comes at a cost of crosslink density (Smeets, Patenaude et al., 2014). In this context, a polymer with the same benefits as PEG but a more versatile chemistry would be highly beneficial.

Poly(oligoethylene glycol methacrylate) (POEGMA) has proven to be an interesting material that overcomes many of the challenges faced with using PEG. This polymer has a carbon-carbon backbone with a PEG side chain of variable length. While POEGMA possesses all of the key desirable biological properties of PEG (i.e. low protein adsorption, low cell adhesion, minimal immune response, etc.), it also has other beneficial features. First, by controlling the PEG side chain length, it is possible to vary the LCST between 26 and 90°C, thereby introducing thermoresponsivity to the polymer (Lutz,

*Polymer Science*, 2008). Similar observations describe varying polymer LCST values between 19 and 40°C by balancing the statistical ratio of short-chain (more hydrophobic) and long-chain (more hydrophilic) monomer components, akin to variation in PEG chain length (Tai et al., 2013; Jia et al., 2006). As previously mentioned, a widely used thermoresponsive polymer is PNIPAM (Lin et al., 2009). With a LCST around 37°C, the porous network is receptive to changes in temperature, allowing for controlled payload release *in vivo*. Moreover, since this response is reversible, cellular attachment and detachment can also be controlled in a switchable manner. Relative to PNIPAM, the monomer of which is quite toxic and has complicated regulatory approval, the OEGMA monomers used to prepare POEGMA are much less toxic, providing an opportunity for POEGMA to be used as a safer alternative to PNIPAM (Smeets, Patenaude et al., 2014). By varying the side chain length and, hence, LCST of POEGMA, it is possible to produce a polymer that can act more like PEG, PNIPAM, or some combination of both.

Second, the ease with which POEGMA can be synthesized and functionalized offers another key benefit of this polymer. The polymerization technique most frequently used to make this polymer is facile, one-step free radical polymerization, allowing for regulation of polymer size, composition, structure, and functionality (Bakaic, Hoare et al., 2015). Controlled free radical techniques can also be used to prepare polymers with well-defined molecular weights. Moreover, the ease of copolymerization in free radical polymerization provides the opportunity to incorporate a wide variety of functional groups into the POEGMA polymer precursors including both chemical and biological cues to enhance the hydrogel properties and reactive sites for crosslinking (Bakaic, Hoare

et al., 2015). The composition of the functionalized polymer will ultimately determine how the hydrogel network is formed (i.e. physical or chemical crosslinking) and the physicochemical properties of that system. Our group has reported extensively on the functionalization of separate POEGMA precursors with aldehyde and hydrazide groups to allow for the formation of labile hydrazone bonds in hydrogel development, as shown in Figure 1.1.

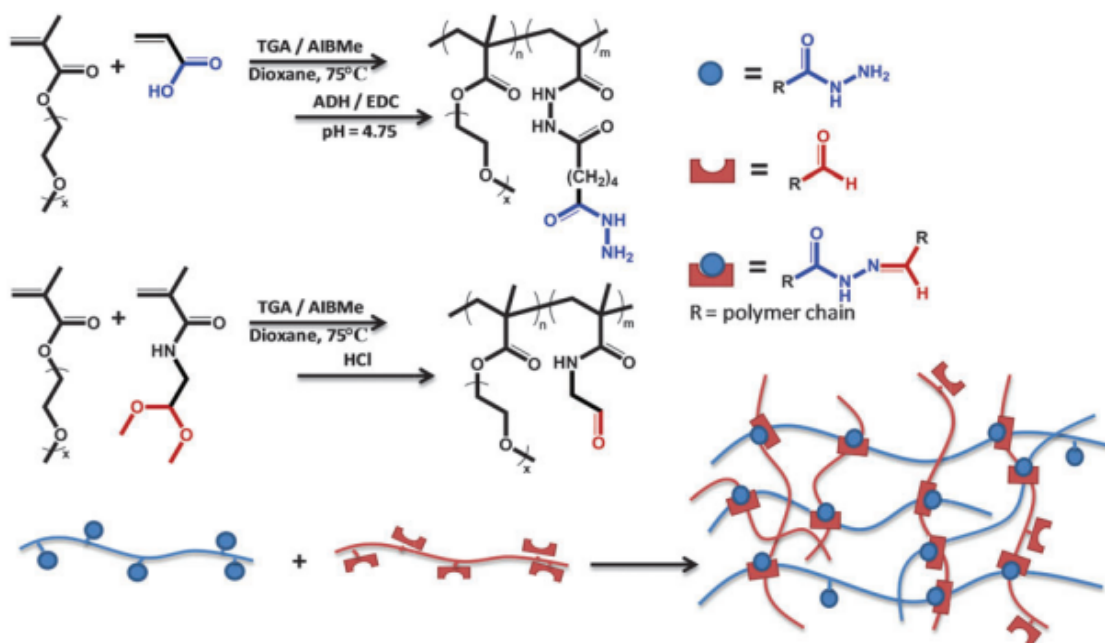


**Figure 1.1.** Typical synthesis of POEGMA polymer precursors and hydrogels using hydrazone chemistry. Image adapted from the literature (Smeets, Bakaic et al., 2014).

The use of this POEGMA platform provides a multitude of benefits for the development of a biomaterial with applications in drug delivery and tissue engineering among many others. By incorporating hydrazone chemistry into the system, we provide a functionally diverse platform that can be crosslinked within seconds to minutes following

simple mixing, facilitating *in situ* gelling with no need for external temperature, UV, or small molecules to cure the hydrogel. This means that it is possible to maintain an injectable system that can deliver polymer precursors directly to the site of interest for optimal therapeutic effect. Moreover, the use of an injection is ideal in a clinical setting as it reduces discomfort, chance of infection, time for recovery, and overall cost (Bakaic, Hoare et al., 2015; Choi et al., 2015; Prestwich, 2007). Overall, POEGMA offers the benefit of low cytotoxicity, low protein adsorption, potential thermoresponsive aspects, and highly versatile functionality (Lutz, 2011). It can be synthesized using facile methods and, by functionalization with reactive aldehyde and hydrazide groups, an injectable and *in situ* gelling system is easily achievable. While more work needs to be done towards developing a marketable product for clinical use, POEGMA is a promising platform that can be used in the modular design of highly tunable hydrogels.

### **1.3. Hyperbranched Polymers**

Introducing structural variation into a polymer network is a popular method of enhancing hydrogel properties as well as providing another platform for tunability (Hadjichristidis et al., 2001). While there are many architectures that have been explored (for example, see Figure 1.2), dendritic formations are some of the most prominent structures used (Mintzer et al., 2011; England et al., 2010). Dendrimers are tree-like polymers that are comprised of a multi-functional small molecule core and multiple generations of branches extending outwards in a symmetrical fashion. Due to the excellent control over the polymer growth and structure, populations of dendrimers are nearly monodisperse and highly compact. Moreover, the branched structure permits

orientation of a high density of functional groups within the polymer structure, especially at the periphery, which enables their use in a wide array of biomedical applications (Abbasi et al., 2014; Tomalia et al., 2002).

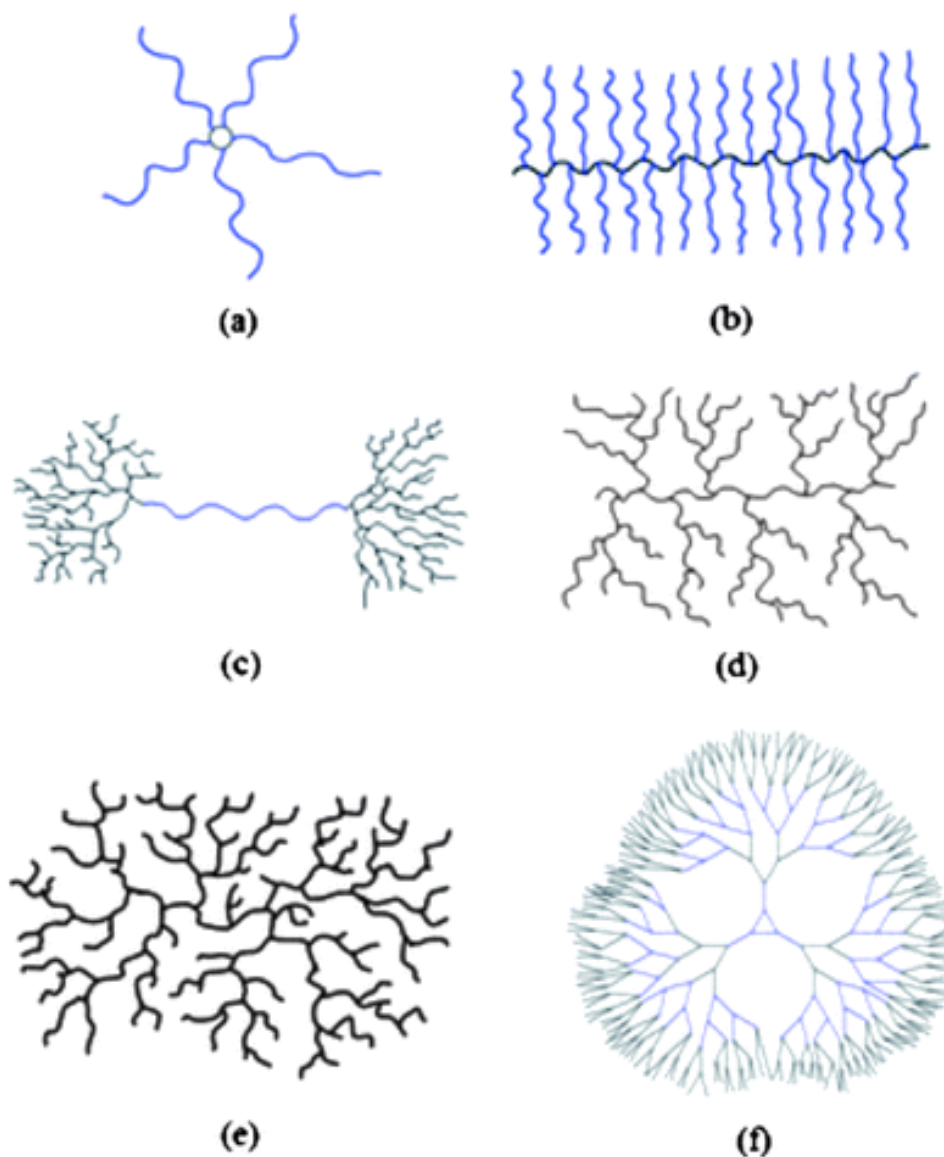


**Figure 1.2.** Schematic of various branched polymer architectures - (a) star, (b) brush or comb, (c) “pom-pom”, (d) dendigraft, (e) hyperbranched, and (f) dendrimer. Image adapted from the literature (England et al., 2010).

Several researchers have applied functional dendrimers as building blocks for hydrogel matrices. Joshi and Grinstaff described the use of dendritic poly(amidoamine) and poly(propyleneimine) as components of tissue engineered scaffolds, specifically for use as a crosslinker. These scaffolds showed greater mechanical strength, improved biological properties in terms of their ability to display a multitude of bioactive factors, and decreased swelling in comparison to those made with a typical linear crosslinking agent (Joshi et al., 2008). By adding bioactive markers such as folate to the dendrimer end-groups or complexing the structure with another compound such as DNA, other groups have shown that dendrimers can be useful to target tumours or to deliver genes for transfection (Chen et al., 2008; Fu et al., 2008). To achieve better stability *in vivo* as well as improved hydrogel properties and pharmacokinetics, for instance, other research groups have incorporated PEG of varying chain lengths into the dendrimer hydrogel system (Kojima et al., 2011; Desai et al., 2010). However, despite the demonstrated advantages of such dendrimers as hydrogel building blocks, dendrimers do not seem to be the ideal biomaterial for use in the clinic. First and foremost, the degree of complexity and monodispersity of dendrimer synthesis means that the cost is increased substantially over other polymer materials, particularly given the laborious multi-step synthesis consisting of multiple high yield reaction/deprotection steps. Second, even though dendrimer end-groups can be highly functionalized, properties like solubility can become an issue when any significant amount of drug is conjugated onto the dendrimer branches. Therefore, the carrier-to-active weight ratios of drug-loaded dendrimers are typically quite low, which is a deterrent for industrial development. Lastly, there are alternative

carriers that are currently being studied or used in the clinic that perform much better than comparable dendrimer compounds and cost a fraction of the price. For example, phosphatidylcholine liposomes and poly(D,L-lactide-*co*-glycolide) (PLGA) nanoparticles exhibit superior drug loading capacities and similar drug release profiles and cytotoxicity as poly(amidoamine) dendrimers (Svenson, 2015). Therefore, a better option may be to find a polymeric alternative that is easily synthesized, readily available, and low-cost, even if that means sacrificing perfectly structured compounds (Voit et al., 2009).

One of those alternatives is hyperbranched polymers, a dendrimer-like structure but with random rather than symmetrical branching. While a few of these compounds are already commercially available (i.e. Hybrane® - polyester amide, Boltorn® - polyester, and Polymin® - polyvinylamine, all used as resins for coatings and flocculants), most hyperbranched materials are still at the research phase in terms of identifying optimal and controllable synthesis techniques as well as developing tunable polymer platforms for customized use (Svenson, 2015). However, among these examples, hyperbranched polymers appear to exhibit many of the same key properties as dendrimers as hydrogel building blocks (albeit with somewhat more polydispersity) while greatly expanding the potential scope of compositions accessible in a highly branched form. In particular, hyperbranched polymers can be designed from a range of different smart materials, with the hyperbranched morphology shown to significantly impact the environmentally responsive properties of the resulting materials. For example, Luzon et al. described a thermoresponsive hyperbranched POEGMA system with the polymer precursors having variable LCSTs based on monomer composition, but also found that the this transition

point was decreased by 5 to 10°C compared to linear analogues prepared with the same composition (Luzon et al., 2010). This may be attributed to the hyperbranched polymers having branches that maintain close proximity between the thermoresponsive units in the swollen state. This would promote a higher cooperativity between functional groups during phase transition, thus leading to a lower effective temperature being required to drive the physical transition (Luzon et al., 2010; Liu et al., 2007).

Analysis of hyperbranched polymers began in the late 1980s, starting with the production of materials such as hyperbranched polyester via polycondensation (Tomalia et al., 2002; Gunatillake et al., 1988). Since then, methods of synthesis have been divided into three main categories: bottom-up, middle-upon, and top-down. The latter two approaches involve grafting medium sized pieces together or degrading much larger molecules (including pre-formed gels) to reach the “hyperbranched” state at a reasonable size (Liu et al., 2013; Esfand et al., 2001). A much more commonly utilized technique is bottom-up synthesis, where monomer(s) are polymerized together with an appropriate initiator or catalyst (Yan et al., 2011). This approach to hyperbranched polymer synthesis covers a variety of polymerization techniques including step-growth polycondensation, ring-opening polymerization, free radical polymerization, atom transfer radical polymerization (ATRP), and reversible addition-fragmentation chain transfer (RAFT) (Luzon et al., 2010; Yates et al., 2004). Each of these has their own specific requirements (i.e. monomer types and reaction conditions), advantages, and disadvantages.

Step-growth polycondensations involve multi-functional monomers that are typically polymerized in a one-step process. While the polycondensation technique is

typically facile and performed under moderate conditions, the solution frequently gels during polymerization and more extensive purification may be required to yield the desired product (Yates et al., 2004). Multiple groups have reported the synthesis of hyperbranched polyphosphates and polyphosphoesters via ring-opening polymerizations of cyclic monomers, with functionalization of side chains possible due to the availability of reactive vinyl pendant groups (Tian et al., 2012; Liu et al., 2009). Of particular relevance, Liu et al. described a self-condensing ring-opening polymerization that did not require a catalyst and produced pure material with a high ratio of hydroxyl groups. This particularly allows for further modification and potential application in the biomedical field, albeit still with a high probability of undesired side reactions occurring during production (Liu et al., 2009). Hyperbranched polyglycerols made via ring-opening polymerization have also garnered significant interest for their use in biomedical applications, specifically based on their potential as therapeutic drug and gene delivery vesicles as well as their compatibility with blood and cells *in vitro* (Kainthan et al., 2007; Kainthan et al., 2006). These molecules are hypothesized to mimic proteins in solution due to the compact nature of their structure and their high degree of branching and molecular weight. The branched structure also allows for functionalization of the materials with high peripheral concentrations of biologically active moieties, making them ideal candidates as therapeutic carriers or protein substitutes in nanobiotechnology and nanomedicine applications (Kainthan et al., 2007).

Chain growth polymerizations such as free radical polymerization have also shown promise for the production of hyperbranched polymers. Free radical

polymerizations are defined by three distinct stages: initiation, chain propagation, and termination. In contrast to step-growth reactions, this form of addition reaction is also characterized by monomers having no leaving groups and thus, the polymerization reaction has no byproducts. In addition, any monomer with a vinyl group (e.g. styrenics, acrylates, methacrylates, and other vinyls) can be polymerized to incorporate controlled numbers of a range of other functional groups into the material, making this approach more tolerant to a larger variety of monomer types while decreasing the potential for gelation during the reaction process (Cowie et al., 2008). In most cases, high conversion is observed with this type of synthesis; however, auto-acceleration can become an issue if the reaction is done in bulk phase or more concentrated solutions. Despite the relative lack of control (albeit arguably more control relative to the step-growth materials), this is a relatively easy polymerization technique and can be used with a multitude of monomers (Cowie et al., 2008). O'Brien et al. used this method in the polymerization of methyl methacrylate (MMA) to get a branched polymer structure. Their approach used only readily available materials and was successful in producing more complex polymers on a useful scale at low cost (O'Brien et al., 2000). Lutz and Hoth used a similar method but with oligo(ethylene glycol) methacrylate as the monomer to create POEGMA hyperbranched polymers, a technique that has been built upon in this thesis (Lutz et al., 2006).

While these methods are useful and generally easy to utilize, simple free radical polymerization leads to (1) relatively uncontrolled chain growth, resulting in a significant risk of gelation at higher yields as well as higher batch-to-batch variation and (2) minimal

control over the complex structure of the hyperbranched polymers. Instead, living or controlled radical polymerizations can be used in which polymer growth or molecular weight increases linearly with conversion as opposed to the exponential growth seen in free radical polymerizations. These reactions are characterized by suppressed termination and chain ends comprised of active radicals (Chanda, 2013). Based on the vinyl group composition of the monomers/polymer, living polymerizations have proven to be more effective for the synthesis of hyperbranched polymers with controllable kinetics (Ishizu et al., 2002). Other benefits of this polymerization approach include first order kinetics based on the monomer, lower polydispersities, and well-defined end groups. Termination of these reactions can occur by coupling or chain transfer of radical chains, which will transpire increasingly as monomer is consumed, or if reactive molecular oxygen is present in the system (Chanda, 2013). Therefore, for a successful reaction, it is essential that all oxygen is evacuated from the reaction vessel and the polymerization is kept under an inert gas (i.e. nitrogen) blanket.

Two of the most widely used living radical polymerization methods for hyperbranched polymer synthesis are atom transfer radical polymerization (ATRP) and reversible addition-fragmentation chain transfer (RAFT) (Chanda, 2013; Zhao et al., 2013). ATRP is similar to typical free radical polymerizations except for the inclusion of a halogenated organic compound and a transition metal, which facilitates chain initiation. Based on the equilibrium with these compounds and growing radical chains, the reaction can be reversibly activated and deactivated, allowing for controlled growth of polymers and thus significantly lower polydispersities (typically between 1.1 and 1.5) (Chanda,

2013). This polymerization method is fairly versatile and compatible with monomers such as styrenes, acrylonitrile, (meth)acrylamides, and (meth)acrylates. One group has used ATRP to synthesize hyperbranched MMA in which was incorporated a thermally labile Diels-Alder linkage to analyze the growth of polymer branches to confirm the structure was prepared in a controlled manner. (Sun et al., 2014). ATRP has also been used to synthesize POEGMA-based hyperbranched polymers that exhibited a cloud point close to physiological temperature; however, ethylene glycol dimethacrylate (EGDMA) crosslinker could only be incorporated up to 10 mol% without experiencing issues with gelation during polymerization and the creation of insoluble networks instead of hyperbranched polymers (Dong et al., 2012; Dong et al., 2010). Moreover, ATRP only allows the use of a select few monomer varieties, typically requires expensive reactants, and necessitates the use of a transition metal catalyst (often copper-based) that can be tedious to remove in subsequent purification steps, especially when using PEG-based materials (Ornelas et al., 2010; Lutz, *Angewandte Chemie*, 2008; Matyjaszewski et al., 2001). In particular, monomers containing acidic functional groups or functional groups with lone pairs of electrons that can complex to the ATRP catalyst must be avoided, limiting the direct utility of ATRP in preparing biologically-relevant functional polymer molecules (Cowie et al., 2008; Ornelas et al., 2010).

RAFT has been able to overcome these limitations with the main advantage being the ability to utilize a wide array of monomer types due to higher functional group tolerance, including those of the acidic variety. While it does require the use of a specialized RAFT agent to ensure that the transfer between chains is regulated, this

approach has been widely adapted to a variety of monomers to produce well-defined polymers with low polydispersities and does not require post-polymerization purification steps as the RAFT agent becomes part of the polymer chain end groups (Ornelas et al., 2010; Chiefari et al., 1998). Moreover, this controlled polymerization slows the reaction kinetics in comparison to standard free radical polymerization; while this may mean longer reaction times, hyperbranched polymers can as a consequence be synthesized to higher conversions without the formation of gels (Luzon et al., 2010). A wide variety of hyperbranched polymers have been synthesized via RAFT including polymethacrylates, polyacrylates, polycarbonates, polyethylenes, polyacrylamides, polystyrenes, and derivatives thereof (Shi et al., 2012; Wang et al., 2010; Xu, Liu et al., 2009; Vogt et al., 2007; Liu et al., *Macromolecules*, 2005; Yates et al., 2004). The key to a successful RAFT polymerization is the effective choice of a RAFT agent based on its compatibility with the monomer(s) to be polymerized. Specifically, the compound must be comprised of a thiocarbonylthio group that contains a good free radical leaving group and an activating group. One significant observation about these reactants is that using dithiobenzoate compounds appears to slow the polymerization kinetics when using acrylate, methacrylate, or styrene monomers. Moreover, the choice of RAFT agent can directly affect functionalization potential based on the composition of polymer chain end groups introduced by the RAFT agent both during and at the end of polymerization (Moad et al., 2005). In our POEGMA system, 2-cyano-2-propyl-4-cyanobenzodithioate (CPCBD) was deemed to be the most ideal RAFT agent based on its demonstrated compatibility with methacrylate monomers (Chin et al., 2014).

The mechanism of RAFT (shown schematically in Figure 1.3) is characterized by six distinct polymerization stages: initiation, propagation, RAFT pre-equilibrium, reinitiation, RAFT main equilibrium, and termination (Chanda, 2013; Cowie et al., 2008). Polymerization begins when a thermal initiator, such as azobisisobutyronitrile (AIBN), decomposes into radical fragments. Chain growth occurs as these radical fragments react with monomer species to form an active propagating sequence. At some point the RAFT agent will connect with a radical chain and form an intermediate that is in a dynamic equilibrium with the previous species or a polymer chain/RAFT agent species and a radical. However, the radical group in this intermediate structure is generally a good leaving group and can dissociate to react with another monomer, effectively forming a new radical chain. At this point there is a rapid interchange between species, forming intermediate structures where the radical molecules are shared equally. Once the monomers have mostly been used, the radical polymer chains increasingly react together to form a “dead” polymer chain that is no longer living. Termination may also occur if reactive oxygen is introduced into the system (Cowie et al., 2008; Moad et al., 2005). These latter two steps are undesirable for maintaining low dispersities, requiring reactions be conducted to <100% conversions and under an inert atmosphere to facilitate the production of highly controlled polymer structures.

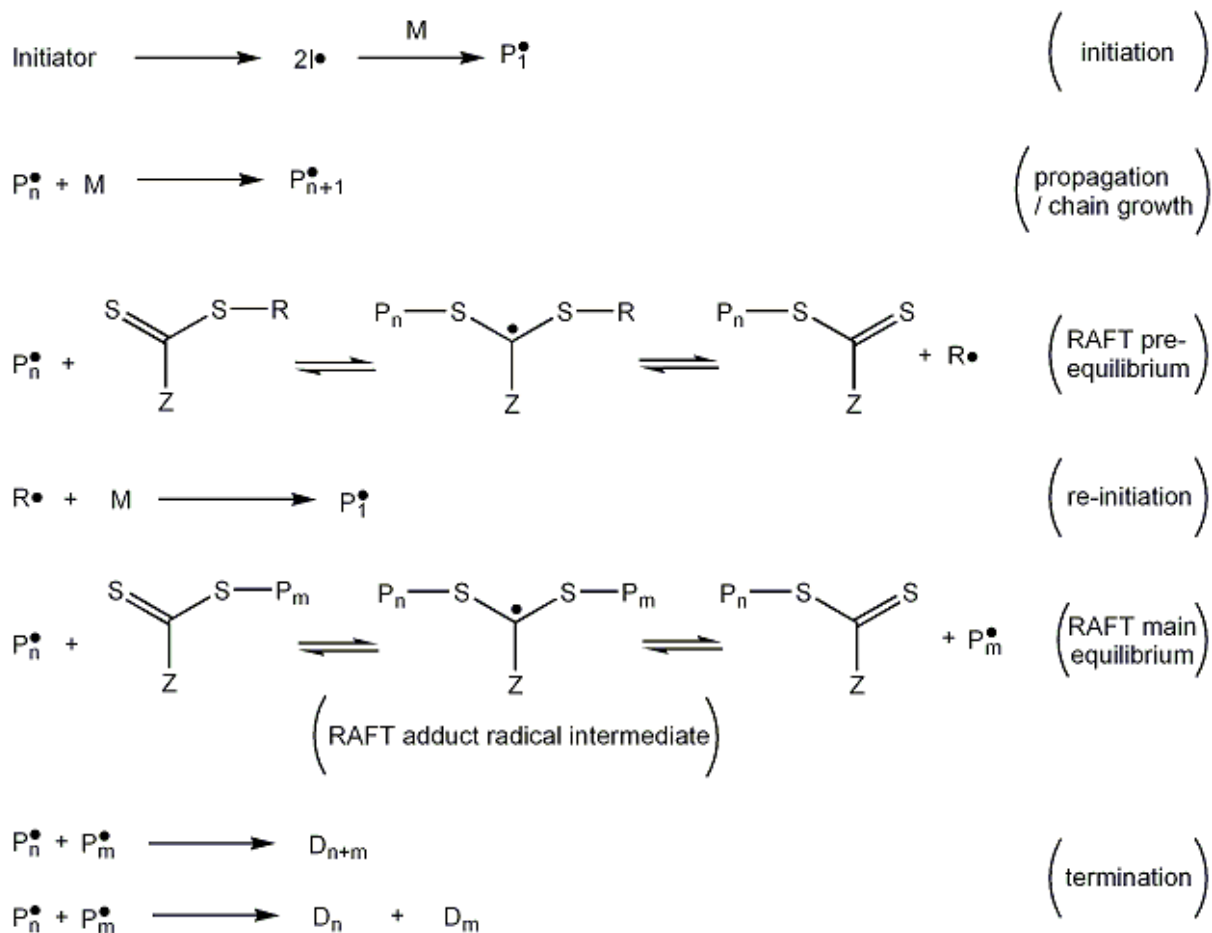


**Figure 1.3.** General mechanism of reversible addition-fragmentation chain transfer (RAFT) polymerization. Image adapted from the literature (Cowie et al., 2008).

Numerous groups have investigated the use of RAFT for the synthesis of hyperbranched polymers, focusing on identifying the optimal reactant compositions, reaction conditions, and potential applications. Alfurhood et al. investigated the synthesis of hyperbranched poly(N-(2-hydroxypropyl) methacrylamide) and showed that increasing the amount of initiator increases the monomer conversion while varying the monomer to RAFT agent ratio facilitates tuning of the polymer cloud point (Alfurhood et al., 2016). Isaure, Cormack, and Sherrington compared the effects of the crosslinkers EGDMA,

ethylene glycol diacrylate (EGDA), and divinylbenzene (DVB) on hyperbranched polymer synthesis. DVB produced more regular branches and low PDIs and EGDMA could be incorporated most efficiently based on the calculated chain transfer constant, while EGDA resulted in a high amount of unreacted pendant groups that made it the least effective crosslinker (Isaure et al., 2004). On this basis, as well our knowledge from previous work and its structural similarity with the OEGMA monomer units, EGDMA was chosen to be the crosslinker in our hyperbranched POEGMA system. In terms of reaction conditions, Liu et al. found that polymerization kinetics were accelerated with temperature and crosslinker concentration but retarded with RAFT agent concentration, consistent with expectations based on the mechanism. Moreover, the ratio of monomers to initiator can greatly impact the reaction rate as well as the resulting polymer size and dispersion (Liu et al., *Polymer*, 2005). Further modifications of the basic RAFT technique in the synthesis of hyperbranched polymers have been pursued with varying degrees of success. Wang et al. used a semi-batch method in which they fed in monomer on a continuous basis over the reaction period. While they did achieve high conversions, the polydispersity ranged from 4.7 to 8.6, indicating a potentially uncontrolled polymerization and subsequent polymer structure (Wang et al., 2010). Xu et al. synthesized hyperbranched poly(methyl acrylate) and PNIPAM using RAFT with a dithiobenzoate RAFT agent whose resulting end groups were subsequently cleaved via aminolysis to form thiol groups that could be further functionalized with bromoesters in a thio-bromo “click” reaction (Xu, Boyer et al., 2009).

#### **1.4. Hyperbranched Polymer Assemblies and Hydrogels**

Based on the literature, it is clear that the polymer network structure has a major impact on the properties of the polymer building blocks as well as the subsequent superstructures made of these materials (Jin et al., 2012; Voit et al., 2009). This is evident in numerous natural systems, such as proteins, where the distinct folding pattern and overall shape determines how the protein will function in its native pathways. By controlling the degree of branching of a polymer, different internal structures can be produced (akin to different protein secondary structures). Jin et al. designed a self-assembling amphiphilic hyperbranched polymer in which they varied the degree of branching (DoB) to make model membranes. By changing the extent of branching within the polymer network, significant changes in the morphology of the overall polymer structure were observed. For instance, they found that a brush conformation produced spherical micelles, slight branching produced tubes and rods, and hyperbranching produced double membrane vesicles (Jin et al., 2012). Therefore, making these small changes in internal structure can give rise to significantly different systems with different properties that can be utilized in a wide array of applications. Further evidence to this is work done by Zhang et al., who synthesized poly(amidoamines) with variable DoBs as precursors for hydrogels to be utilized as DNA carriers for gene therapy. Low-branched structures had higher transfection efficiency, cellular uptake, and DNA binding compared to either linear or more highly branched polymers (Zhang, Ma et al., 2013). The high density of surface functional groups (whose identity is tunable based on the nature of the chain transfer

agent used) also facilitates the conjugation of different bioactive molecules with different target functions (Wang et al., 2015).

By crosslinking hyperbranched polymers together to create hydrogels, the unique properties of the hyperbranched polymer building blocks can be leveraged to create hydrogels with highly tunable properties that have been explored in a variety of biomedical applications. In particular, the nanoscale properties of hyperbranched polymers maintain the quality of injectability, making them ideal for drug/gene delivery vesicles in the clinic (Luzon et al., 2010). Other groups have successfully synthesized hyperbranched POEGMA via RAFT and found that the crosslinking/branching conditions altered the gelation and mechanical properties so as to enhance the hydrogel functionality in applications such as cell delivery and tissue engineering scaffolds (Dong et al., 2015; Tai et al., 2015; Kennedy et al., 2014). PEG-HA and other PEG-based hyperbranched hydrogel systems have also been reported that were attractive carriers for drugs, genes, cells, and other diagnostic and/or therapeutic payloads (Ardana et al., 2014; Hassan et al., 2013; Gao et al., 2004). Lui et al. developed a hyperbranched phosphoramidate-hyaluronic acid hybrid that was injectable and showed controlled release of bovine serum albumin (BSA) over time as well as tunable mechanical and degradation properties (Lui et al., 2015). Photocrosslinked hyperbranched polyglycerols have also been developed that exhibit low degrees of swelling, indicating a stable network that can be useful in applications such as drug delivery and tissue engineering (Oudshoorn et al., 2006). Along the same lines, hyperbranched polyglycerol microgels were prepared using micromolding techniques that could be used for similar applications (Oudshoorn et al., 2007). Zhang et

al. found that hyperbranched polyester hydrogels had a high capacity for bioactive therapeutics due to their globular and hydrophobic inner nanostructure. By changing the crosslink density within the network, they were also able to control mechanical strength (i.e. compressive modulus) of the hydrogels. Furthermore, cell adhesion, spreading, and proliferation on the hydrogel surface were tunable based on the polymer and hydrogel composition (Zhang, Patel et al., 2013). Hybrid hyperbranched poly(ether amine) hydrogels have also been developed that are able to adsorb guest dyes selectively based on differences in adsorption capacities and kinetics for various dyes, which has potential for applications in dynamic separation of dye mixtures (Deng et al., 2012). Lastly, Corneillie and Smet reported the introduction of branching into poly(lactic acid) (PLA) in order to overcome limitations in polymer strength, toughness, and lack of free functional groups inherent to linear PLA (i.e. only on chain ends). Hydrogels made from mixing these biopolymers with other compatible biopolymers such as chitosan exhibited enhanced properties, yet maintained their biodegradable qualities, providing further opportunities for use while decreasing the amount of waste material (Corneillie et al., 2015). Therefore, introducing complex architectures such as hyperbranching into hydrogel precursor polymers allows for enhanced hydrogel properties and provides a separate platform for tuning those properties.

While the DoB has been investigated in terms of the hyperbranched polymers alone, minimal attention has been paid to the properties of the hydrogels prepared using these building blocks. Thus, we have designed this study to try and fill that gap. By combining the structural effects of hyperbranching with our previously defined POEGMA

platform, we hope to develop a hyperbranched hydrogel system that is highly tunable while maintaining the desirable biological properties of this polymer, as previously described. Figure 1.4 depicts the scheme for our chosen polymerization method. Based on all of the arguments made up to this point, it was decided to use OEGMA and MAA as the functional monomers, EGDMA as the divinyl crosslinker or branching agent, and CPCBD as the RAFT agent, along with a thermal initiator, AIBN.

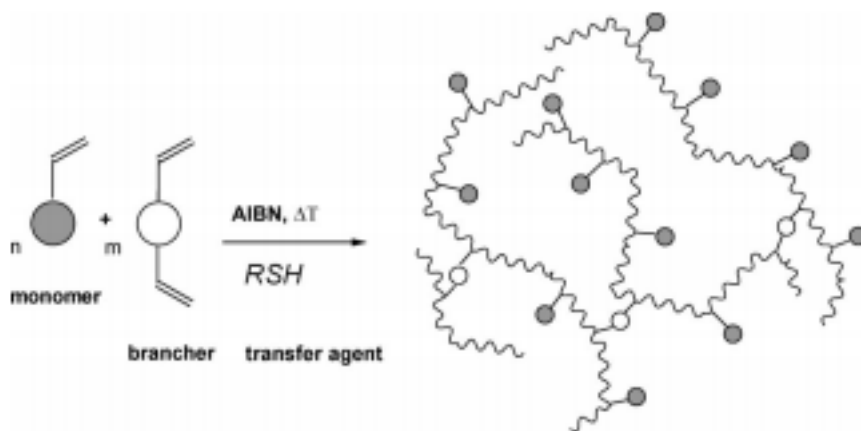


**Figure 1.4.** Scheme of hyperbranched polymer synthesis using RAFT. For this project, the functional “monomers” were OEGMA and MAA, the “brancher” was EGDMA, the initiator was AIBN (as shown), and the “transfer agent (RSH)” or the RAFT agent was CPCBD. Image adapted from the literature (Voit et al., 2009).

Herein, we investigate the gelation kinetics, mechanical properties, degradation and swelling kinetics, cytotoxicity, and protein adsorption of hyperbranched POEGMA hydrogels using the aforementioned polymerization approach. This thesis will focus on the effects of the degree of branching within the polymer precursors and highlight the differences between the properties of hyperbranched-linear and hybrid hyperbranched-hyperbranched systems. We anticipate these differences in properties achieved using hyperbranched polymers will offer significant potential in effectively tuning the

M.A.Sc. Thesis – H. Dorrington; McMaster University – Chemical Engineering

properties of *in situ* gelling hydrogels while only minimally manipulating the underlying chemistry of the materials.

## **Chapter 2 – Hydrogels Prepared with Hyperbranched Building Blocks**

### **2.1. Introduction**

Hydrogels have been the focus of significant research in the areas of biomedicine and bioengineering for many years due to their similarities with native extracellular matrices and their ability to supplement and replace diseased or damaged tissue (Aziz et al., 2015). By varying the chemical composition, it is possible to create a hydrogel with characteristics that are similar to those of a wide array of soft tissues (Levental et al., 2007). Moreover, by tuning the porosity of the networks, controlled transport of materials in and out of the network is facilitated, which is ideal for applications in tissue engineering as scaffolds for tissues and organs as well as regenerative medicine, drug delivery, gene therapy, cellular immobilization, and many others (Gaharwar et al., 2014; Wu et al., 2008).

To ensure that these materials are clinically relevant, significant effort has been invested in designing *in situ*-gelling or injectable hydrogels, allowing for the reduction of discomfort, risk of infection, recovery time, and overall cost for patients (Prestwich, 2007). While both physical and chemical crosslinking can be utilized in hydrogel formation, physical interactions can be difficult to control, particularly in terms of regulating degradation times, the highly diluting, and aggressive *in vivo* environment (Patenaude et al., 2014; Chen et al., 2004). Therefore, although the introduction of functional chemistry can pose some potential challenges with biocompatibility, chemical crosslinking offers the potential for making hydrogels with much more tunable

physicochemical properties. To this end, a number of chemistries have been investigated to form *in situ* gelling covalent bonds, including Michael-type addition, disulfide bridges, hydrazone condensation, and Diels-Alder cycloaddition, among others (Patenaude et al., 2014). While the type of chemistry used depends on the polymer precursors and the functional groups thereof, it is also dependent of the needs of the application in terms of gelation time, degradation rate, and potential byproducts from both bond formation and hydrogel degradation. Hydrazone chemistry has proven to be an attractive option due to the fast and controllable gelation kinetics (on the order of a few seconds to a few minutes) as well as the hydrolytically labile nature of the bond, making it readily degradable over weeks-to-months at physiological pH in the *in vivo* environment (Patenaude et al., 2014).

While many natural and synthetic polymers have been studied for use in the production of hydrogels, poly(ethylene glycol) (PEG) and poly(N-isopropylacrylamide) (PNIPAM) have both garnered significant amounts of attention. PEG has been approved by the Food and Drug Administration (FDA) for several *in vivo* applications based on its non-immunogenic and non-cytotoxic properties and is well established to resist the adhesion or adsorption of cells and proteins (Smeets, Bakaic et al., 2014; Peppas et al., 1999). However, PEG is inherently limited as a biomaterial based on its inherent lack of functional group availability (i.e. only chain ends are available for both functionalization and crosslinking), resulting in hydrogels with relatively low mechanical strength, high swelling ratios, and weak drug-hydrogel interactions (Smeets, Patenaude et al., 2014). In contrast, PNIPAM is an attractive polymer for applications in drug delivery by virtue of its thermoresponsive nature, with a lower critical solution temperature (LCST) around

physiological temperature. However, while several papers have reported excellent cytocompatibility of PNIPAM in a variety of applications, the monomer is highly toxic and the degradation products, if they exist, cannot be firmly characterized, making their approval for use in *in vivo* applications challenging (Lin et al., 2009).

More recently, poly(oligoethylene glycol methacrylate) (POEGMA) has been demonstrated to offer the potential to combine the desirable biological and thermoresponsive traits of both PEG and PNIPAM. By varying the number of repeat units in the ethylene glycol side chain ( $n$ ), the LCST can be tuned and the polymer can exhibit characteristics close to that of PEG ( $n > 7-8$ ) or closer to PNIPAM ( $n \sim 2-3$ ) (Lutz, 2008). In addition, as a polymer prepared by free radical polymerization instead of step growth polymerization, any number of reactive side chain comonomers can be incorporated to introduce controlled degrees of functionalization in the polymer by simple statistical copolymerization, overcoming a key limitation of PEG.

Our group has recently reported extensively on injectable POEGMA-based hydrogels which exploit the potential for POEGMA functionalization, in this case with hydrazide and aldehyde functional groups, to create an *in situ*-gelling hydrogel based on hydrazone chemistry that does not require the use of UV, temperature, or small molecules for crosslinking. The kinetics of labile hydrazone bond formation (on the order of a few seconds) also promotes the use of these polymer precursors in an injectable system. The properties of POEGMA hydrogels can be tuned by varying the polymer precursor composition, concentration, or reactive functional group content and/or by introducing functional ligands, peptides, and other moieties to direct specific cell or drug interactions

with the hydrogel (Bakaic, Hoare et al., 2015). However, there are still challenges with these materials in terms of (1) producing PEG-like materials (i.e. with longer side chains) with stronger mechanics capable of mimicking stiffer soft tissues like cartilage and (2) avoiding the need to significantly change the polymer chemistry (i.e. the number of reactive functional groups in the polymer) to effect significant changes in the subsequent hydrogel properties. Of note, developing hydrogels that have distinct mechanical properties but similar chemistries offers particular potential in elucidating how cells respond to substrates of varying stiffnesses without the confounding potential impacts of interfacial chemistry.

One method of overcoming these constraints is to change the physical morphology of the polymer precursors as opposed to their chemistry. In particular, introducing hyperbranching into polymer networks, as characterized by the inclusion of a crosslinking or branching agent to produce tree-like structures with random branching (see Figure 1.2), has potential to significantly change the physical, mechanical, and biological properties of hydrogels while introducing minimal chemical variation into the network relative to linear precursor polymers prepared with the same monomer (Corneillie et al., 2015; Zhang, Patel et al., 2013). Such polymers can still be synthesized via facile free radical and living polymerizations, although careful control over the balance of chain branching (crosslinking) and chain end generation (chain transfer) must be achieved to avoid producing either low-branched polymers with similar properties to linear polymers (at low crosslinker content) and/or bulk gels instead of hyperbranched polymer globules (at higher crosslinker and/or lower chain transfer agent content) (Yates

et al., 2004). In order to improve the control over the structure and size of these polymer precursors, many groups have applied controlled radical polymerization-based synthesis techniques such as atom transfer radical polymerization (ATRP) and reversible addition-fragmentation chain transfer (RAFT), both of which have been widely demonstrated to facilitate the production of more well-defined hyperbranched structures (Cowie et al., 2008). While ATRP is able to produce well-defined polymers, this technique is somewhat limited in terms of copolymerizing acidic monomers that can deactivate the ATRP catalysts (Cowie et al., 2008). On the other hand, RAFT is more tolerant of a wide variety of monomers, including acidic ones, and produces well-defined polymers using polymerization conditions similar to those of conventional free radical techniques (Moad et al., 2005).

Hydrogels prepared using hyperbranched polymer building blocks produced with controlled radical methods have significant benefits in terms of physicochemical properties over linear polymer-based hydrogels with similar compositions, including enhanced mechanical strength, higher drug loading capacities, and elongated drug release profiles (Corneillie et al., 2015; Lui et al., 2015; Svenson, 2015; Zhang et al., 2013; Wang et al., 2015; Tomalia et al., 2002). However, little work has been done to determine the specific effects of polymer structure (i.e. branching degree and polymer size) in terms of tuning the properties of the resulting hydrogels, particularly in the context of *in situ* gelling hydrogels in which optimization of the mechanics, gelling time, and degradation is of key importance for their ultimate application. Herein, using the hydrazone-crosslinkable POEGMA platform as the base polymer, we describe how changing the

degree of branching (including zero-branching/linear polymers) and size of a hyperbranched building block affect the properties of hydrogels based on such building blocks. To ensure controlled kinetics during synthesis, the RAFT technique was employed as it also allows the use of both methacrylate and acidic monomers while maintaining an improved level of structural control relative to free radical techniques. In order to target the degree of branching (DoB) of the hyperbranched network, varying amounts of the crosslinker ethylene glycol dimethacrylate (EGDMA) were incorporated into the polymer precursors. A series of hydrogels was then synthesized with the DoB of the precursors ranging from 0 (linear) to 15%. The gelation times, mechanical strength, swelling and degradation kinetics, and biological properties were then analyzed to highlight the key differences between linear-linear, hyperbranched-linear, and hyperbranched-hyperbranched hydrogel systems with largely similar chemical compositions but significantly different internal structures. In particular, we aim to show how varying the structure of polymer precursors can impart significant changes in the resulting hydrogel properties, providing another strategy for tuning hydrogels to suit the needs of the specific application while minimally changing the underlying chemistry of the gel.

## **2.2. Materials and Methods**

### **2.2.1. Materials**

Oligo(ethylene glycol) methyl ether methacrylate with an average molecular weight of 475 g/mol (OEGMA<sub>475</sub>, 95%, Sigma Aldrich), methacrylic acid (MAA, 99%, Sigma Aldrich), and ethylene glycol dimethacrylate (EGDMA, 98%, Sigma Aldrich)

were purified in a column of basic aluminum oxide (type CG-20, Sigma Aldrich) to remove all inhibitors. 2-cyano-2-propyl-4-cyanobenzodithioate (CPCBD, 98%, Sigma Aldrich), azobisisobutyronitrile (AIBN, 98%, Sigma Aldrich), adipic acid dihydrazide (ADH, 98%, Alfa Aesar), *N*'-ethyl-*N*-(3-dimethylaminopropyl)-carbodiimide (EDC, commercial grade, Carbosynth), *N*-hydroxysuccinimide (NHS, 98%, Sigma Aldrich), and aminoacetaldehyde diethyl acetal (ADA, 98%, Sigma Aldrich) were all used as received. Anhydrous (reagent grade) 1,4-dioxane, ethyl ether, and dichloromethane were all purchased from Caledon Laboratories. Deuterated dimethyl sulfoxide (DMSO- $d_6$ ) was purchased from Aldrich Chemistry. Hydrochloric acid (HCl, 1 M) was received from LabChem Inc. (Pittsburgh, PA). For cell viability assays, 3T3 mouse fibroblasts were used (ATCC – Cedarlane Laboratories, Burlington, ON). Media for the cells contained Dulbecco's Modified Eagle Medium – high glucose (DMEM), fetal bovine serum (FBS), and penicillin streptomycin (PS). Trypsin-EDTA (Invitrogen Canada, Burlington, ON), resazurin sodium salt (BioReagent grade, Sigma Aldrich), 5-FITC (>90%, Sigma Aldrich), and 5-FTSC (80%, Sigma Aldrich) were used as received. 5-fluorescein isothiocyanate-labelled bovine serum albumin (FITC-BSA) was prepared as previously described (Bakaic, Dorrington, et al. 2015). Briefly, 50 mg of BSA was dissolved in 100 mL of 0.1 M carbonate buffer (pH = 9), followed by the addition of 1 mg of FITC. The solution was incubated under magnetic stirring at room temperature for 12 hours, dialyzed for 6 cycles (6+ hours each) using a 3.5 kDa molecular weight cut-off regenerated cellulose tubing against a large excess of DI water, then lyophilized. Water used in all experiments was Milli-Q grade.

### 2.2.2. Polymer Synthesis

Hyperbranched POEGMA polymers were synthesized by dissolving OEGMA, MAA, EGDMA, AIBN, and CPCBD in 25 mL of 1,4-dioxane in a 50 mL Schlenk flask. Varying mol% of EGDMA were added based on the DoB being targeted, with the mol% of OEGMA being adjusted accordingly to maintain a fixed MAA content in the resulting polymers. All recipes are shown in Table 2.1. After degassing via three cycles of freeze-pump-thaw, the flask was backfilled with nitrogen, sealed, and placed into a preheated oil bath at 70°C. The reaction was allowed to proceed for 9 or 10.5 (for HBP<sub>H15</sub>) hours under magnetic stirring, after which the reaction was stopped by exposure to air. Dioxane was removed by precipitation in 10x volume excess of cold ethyl ether. Once all solvent was removed, the polymer was ready for functionalization. The number (denoted as X) in the HBP<sub>H/A</sub>X name of all polymer precursors refers to the theoretical degree of branching or mole fraction of EGDMA from the synthesis recipe.

**Table 2.1.** Synthesis of hyperbranched POEGMA polymer series.

Polymer	OEGMA:EGDMA:MAA [mole fraction]	Monomer+EGDMA: CPCBD: AIBN [mole fraction]	DoB <sub>theoretical</sub> [%]
HBP <sub>H</sub> 15	55:15:30	1:85:300	15
HBP <sub>H</sub> 10	60:10:30	1:85:300	10
HBP <sub>H</sub> 5	65:5:30	1:85:300	5
HBP <sub>H</sub> 0	70:0:30	1:85:300	0
HBP <sub>A</sub> 15	55:15:30	1:85:300	15
HBP <sub>A</sub> 0	70:0:30	1:85:300	0

### 2.2.3. Hydrazide Functionalization

HBP<sub>H</sub>15<sub>22</sub>, HBP<sub>H</sub>15<sub>25</sub>, HBP<sub>H</sub>10, HBP<sub>H</sub>5, and HBP<sub>H</sub>0 hydrazide-functionalized precursors were synthesized by dissolving each respective polymer in 100 mL of DI water and kept under magnetic stirring for the entirety of the reaction. ADH was added in excess (10.03 g), allowed to dissolve, then the pH of the solution was adjusted to 4.75 using 1 M HCl. EDC (3.13 g) was then added and the pH was maintained at 4.75 using 1 M HCl over 5 hours or until the pH was no longer changing. After 6 cycles (6+ hours each) of dialysis using a 3.5 kDa molecular weight cut-off regenerated cellulose tubing against a large excess of DI water, the polymer solution was lyophilized. All precursors were stored at 4°C as 20 wt% solutions in 10 mM PBS unless specified otherwise. All hydrazide-functionalized polymers are denoted with the subscript “H” in the HBP<sub>H</sub>X coding.

### 2.2.4. Aldehyde Functionalization

HBP<sub>A</sub>15 and HBP<sub>A</sub>0 aldehyde-functionalized precursors were synthesized by dissolving each respective polymer in 100 mL of DCM. NHS (1.03 g) and EDC (1.38 g) were added to the solution under magnetic stirring and the reaction was allowed to proceed for 6 hours. At this time, ADA (1.41 g) was added and the solution was stirred for another 24 hours. After removing the DCM via rotary evaporation, the resulting polymer was dissolved in 150 mL of DI water and subsequently dialyzed for 2 cycles (6+ hours each) using 3.5 kDa molecular weight cutoff regenerated cellulose tubing against a large excess of DI water to remove excess reactants. The solution was then transferred to

a round-bottom flask, 50 mL of 1 M HCl was added and allowed to react under magnetic stirring for 48 hours to hydrolyze the acetal groups of ADA to aldehydes. The resulting solution was then dialyzed for 6 cycles (6+ hours each) using 3.5 kDa molecular weight cutoff regenerated cellulose tubing against DI water and subsequently lyophilized. All precursors were stored at 4°C as 20 wt% solutions in 10 mM PBS. All aldehyde-functionalized polymers are denoted with the subscript “A” in the HBP<sub>A</sub>X coding.

### 2.2.5. Polymer Characterization

All polymers were characterized after synthesis and after functionalization using aqueous size exclusion chromatography (SEC), nuclear magnetic resonance (<sup>1</sup>H-NMR), and conductometric titration. To determine polymer conversion as a function of reaction time, crude samples of each polymerization reaction were collected at 2, 4, 6, and 9 (or 10.5) hours post-initiation and characterized via aqueous SEC in 25 mM CHES buffer (pH = 10). The SEC system included a Waters 515 HPLC pump, a Waters 717 Plus autosampler, a Waters 2414 refractive index detector, and three Ultrahydrogel columns (30 cm x 7.8 mm inner diameter; 0 – 3 kDa, 0 – 50 kDa, and 2 – 300 kDa), with a mobile phase of 0.5 M NaNO<sub>3</sub>, 25 mM CHES buffer, and 10 ppm NaN<sub>3</sub> at a flow rate of 0.8 mL/min used for all samples. The resulting elution times were analyzed against a standard of linear PEG with sizes ranging from 106 to 584 kDa, the results of which are shown in Figures S.1 to S.7.

Before and after functionalization, all polymers were analyzed in DMSO-d<sub>6</sub> via <sup>1</sup>H-NMR using a 600 MHz Bruker AVANCE spectrometer. The resulting spectra were

analyzed to determine conversion, monomer incorporation, and DoB. To determine conversion, peaks for the vinyl protons were compared with those for the polymer backbone from a crude sample of the reaction mixture immediately after polymerization completion and conversion calculated based on the signals at  $\delta = 5.6-6$  ppm ( $\text{CH}_2 = \text{CH}$ -, residual vinyl protons) and  $\delta = 1.6-2$  ppm ( $-\text{CH}_2$ -, polymerized monomer units in the polymer backbone) according to Equation 2.1:

$$\text{Conversion} = \frac{0.5I_{1.6-2}}{0.5I_{1.6-2} + I_{5.6-6}} \quad \text{Eq. 2.1}$$

Methods described by Luzon et al. (Luzon et al., 2010) were used to determine the relative incorporations of OEGMA, MAA, and EGDMA (mole fraction) into the polymer from the  $^1\text{H-NMR}$  data. Equations 2.2 – 2.5 were used to determine the DoB of each polymer, where P = pendant groups, M = OEGMA, R = branch points, A = MAA (based on conductometric titration), which all represent integral values. Pertinent peaks from the NMR spectra are represented by the labels f, c, and e in Figure 2.1.

$$f = P \quad \text{Eq. 2.2}$$

$$c = 3M \quad \text{Eq. 2.3}$$

$$E = 4P + 4R + 2M \quad \text{Eq. 2.4}$$

$$\text{DoB} = \frac{R}{P + R + A + M} \times 100\% \quad \text{Eq. 2.5}$$

To determine the degree to which each polymer was functionalized with MAA groups, conductometric titration was used. Hyperbranched polymer solutions with a concentration of 50 mg/mL were prepared for each polymer in 50 mL of 1 mmol NaCl and titrated using 0.1 M NaOH as the titrant both before and after functionalization to

track the number of  $-\text{COOH}$  groups consumed by the hydrazide functionalization reaction (i.e. the % conversion of  $-\text{COOH}$  groups to hydrazide groups).

Cloud point temperatures were determined using a Variant Cary Bio 100 UV-vis spectrophotometer. A temperature ramp in the range of 10 to 90°C at a rate of 1°C/min was performed on 5 mg/mL polymer solutions in 10mM PBS, with measurements taken every 0.5°C.

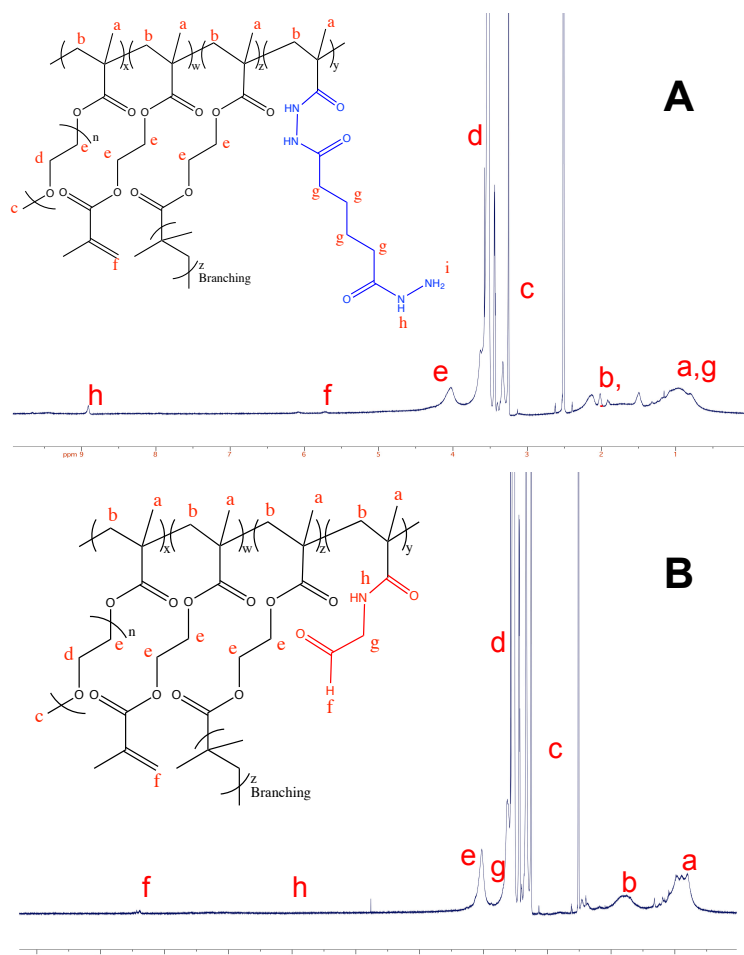


**Figure 2.1.**  $^1\text{H-NMR}$  spectra for  $\text{HBP}_{\text{H}1522}$  (A) and  $\text{HBP}_{\text{A}0}$  (B) hyperbranched POEGMA polymers in  $\text{DMSO-d}_6$ . Note that since  $\text{HBP}_{\text{A}0}$  is a linear polymer prepared without crosslinker – there are no EGDMA or pendant groups present (i.e. side chains w and z in the chemical structure are not represented in the spectrum).

### **2.2.6. Preparation of Hydrogels**

Hydrogels were prepared by pipetting equal amounts of the hydrazide- and aldehyde-functionalized polymer precursors dissolved in 20 wt% solutions in 10 mM PBS into a pre-formed silicone rubber mold, mixing manually by repeated pipetting for 5-10 seconds, and sealing in a container (100% relative humidity) to gel overnight. For swelling and degradation assays, the mold had a diameter of 9 mm and a volume of 250  $\mu\text{L}$ ; for rheology tests, the mold had a diameter of 12 mm and a volume of 400  $\mu\text{L}$ . After extrusion into the appropriate mold, the polymer solution was mixed thoroughly and allowed to gel overnight at room temperature in a sealed container with 100% relative humidity. The gelation time for each of the hydrogels was determined by inversion of a 100  $\mu\text{L}$  (total hydrogel volume) solution in a 2 mL Eppendorf tube (inverted every 30 seconds). Time of gelation was recorded once the gel had ceased flowing when inverted after 30 seconds.

### **2.2.7. Residual Functional Groups Labelling**

Hydrogels were prepared in triplicate to cover the bottom of the wells of a 48-well tissue culture plate by adding 30  $\mu\text{L}$  each of hydrazide- and aldehyde-functionalized polymer precursors at 20 wt% in 10mM PBS, pipetting up and down to ensure solutions were well mixed. Solutions of hydrazide-reactive FITC (0.05 g/L) or aldehyde-reactive FTSC (0.05 g/L) were prepared in carbonate buffer (pH of 8.5). After allowing the gels to equilibrate overnight, 150  $\mu\text{L}$  of one of the reactive fluorescent probes was added in each well. After soaking overnight, all hydrogels were rinsed with fresh carbonate buffer 15

times for 5 minutes each to remove any unreacted probe. After the rinse step, the fluorescence of both plates were measured using a VICTOR 3 plate reader ( $\lambda_{\text{exc}} = 488$  nm and  $\lambda_{\text{emi}} = 535$  nm).

### **2.2.8. Hydrogel Rheology**

Hydrogel discs were prepared as described in section 2.2.6, removed from the molds, and mounted in a parallel plate geometry (12mm diameter) on a Mach-1 Mechanical Tester (Biomomentum Inc., Laval, QC). All tests were performed at room temperature and in triplicate. The compressive moduli were determined by compressing hydrogels to 75% of their original thickness at a rate of 3%/s. Subsequent strain sweep and dynamic frequency sweep tests were performed on these pre-compressed hydrogel discs to determine the shear modulus. For this latter test, discs were first subjected to a strain sweep with amplitudes between 0.1 and 2.2° at 0.5 Hz to find the linear viscoelastic range followed by a dynamic frequency sweep with frequencies between 0.1 and 2.2 Hz and an amplitude within the linear viscoelastic region.

### **2.2.9. Hydrogel Transparency**

In a 96-well tissue culture plate, 30  $\mu\text{L}$  of both hydrazide- and aldehyde-functionalized polymers were added to wells ( $n = 4$ ). Hydrogels were allowed to equilibrate overnight, with the plate being sealed to prevent evaporation. Using a VICTOR 3 plate reader, the absorbance of each gel was measured at a wavelength of 595 nm. Resulting values were compared to measurements of 10 mM PBS (equal volume) as

a control. Using the following equation, absorbance values were converted to transmittance values:

$$A = 2 - \log_{10}(T) \quad \text{Eq. 2.6}$$

Transmittance results are reported as the average of four replicates.

### **2.2.10. Swelling and Degradation Kinetics**

Hydrogel discs, made in triplicate, were prepared as mentioned in section 2.2.6. Once removed from molds, hydrogels were placed in pre-weighed cell culture inserts that were immediately weighed again to determine the initial hydrogel weight ( $W_0$ ). Following, inserts were placed into a 12-well cell culture plate that contained 4 mL of either 10 mM PBS (for swelling assays) or 10 mM HCl (for accelerated degradation assays intended to enable tracking of the relative degradability of different hydrogel compositions). Swelling assays were performed at both room temperature (approximately 22°C) and 37°C. Degradation assays were performed at 37°C. At each sample point, the inserts containing the hydrogels were removed from the plate, the excess PBS or HCl was removed by gentle wicking off of the hydrogel surface, and the inserts/hydrogels were weighed to determine  $W_t$ . The inserts/hydrogels were subsequently placed back in the plates with fresh PBS or HCl in the wells and incubated at the appropriate temperature until the next time point. Assays were complete when the hydrogel had been entirely degraded (as determined visually). Based on the normalized hydrogel weight, the swelling ratio at any time point could be calculated based on the following equation:

$$\text{Swelling Ratio} = \frac{W_t}{W_0} \quad \text{Eq. 2.7}$$

### **2.2.11. Cytotoxicity**

The viability of cells when exposed to each hyperbranched POEGMA polymer was determined using a resazurin cytotoxicity assay following established protocols (Dienstknecht et al., 2010). First, 3T3 mouse fibroblasts were cultured in a 96-well tissue culture plate at a density of 10,000 cells/well, using DMEM (with 10% FBS and 1% PS) as the media. Following pre-incubation at 37°C for 24 hours, polymer solutions with concentrations from 200 to 2000 µg/mL (also in DMEM and sterilized via filtration using a 0.2 µm Pall Acrodisc filter) were added into each experimental well (for a total volume of 50 µL per well) and the plates incubated for another 24 hours at 37°C. Varying amounts of an 8 mg/mL stock solution of resazurin sodium salt in PBS were added to each well, making the final resazurin concentrations 10 µg/mL and the total volume in each well being 250 µL. After incubating for 4 hours at 37°C, the fluorescence of all wells were measured using a VICTOR 3 plate reader ( $\lambda_{\text{exc}} = 531 \text{ nm}$  and  $\lambda_{\text{emi}} = 572 \text{ nm}$ ). Two blank wells of equal volume containing no cells were used to determine background fluorescence, which was subtracted from the value of the experimental wells as a control. To determine relative cell viability, these experimental values were compared to values from control wells containing only cells.

### **2.2.12. Protein Adsorption**

In a 96-well tissue culture plate, 30 µL of both hydrazide- and aldehyde-functionalized polymers were added to wells in repeats of four, pipetting up and down to ensure solutions were well mixed. Hydrogels were allowed to equilibrate overnight, with

the plate being sealed with Parafilm to prevent evaporation. 60  $\mu\text{L}$  of FITC-BSA at concentrations of 125, 250, and 500  $\mu\text{g/mL}$  in 10 mM PBS was added to the wells. After incubating for 2 hours at 37°C, all wells were rinsed three times with fresh PBS to remove any unbound protein. Using a VICTOR 3 plate reader, the fluorescence of all wells was measured and the values were compared to the standard FITC-BSA solution controls of the same concentrations ( $\lambda_{\text{exc}} = 488 \text{ nm}$  and  $\lambda_{\text{emi}} = 535 \text{ nm}$ ).

## 2.3. Results and Discussion

### 2.3.1. Polymer Characterization

A series of hyperbranched POEGMA polymers was synthesized using the controlled RAFT polymerization technique according to the recipes found in Table 2.1. The only variation between polymers was the amount of EGDMA crosslinker that was incorporated, adjusting the OEGMA monomers as required to achieve the desired mole fractions of monofunctional:bifunctional comonomer (MAA was maintained at 30 mol%). Given the difunctional nature of EGDMA, each EGDMA residue incorporated represents one potential branch point; as such, by controlling the amount of EGDMA incorporated into the network, it was possible to target varying degrees of branching between 0 and 15%. Based on our own observation as well as those in the literature, any higher incorporation of EGDMA typically led to gelation during polymerization. The nomenclature used is in the form  $\text{HBP}_{\text{A/H}\#}$ , where the “A/H” refers to the aldehyde (A) or hydrazide (H) functionalization of the polymer, and the number (#) represents the targeted degree of branching. In the case of  $\text{HBP}_{\text{H}15}$ , two different polymers were synthesized in which the polymerization was performed for a different periods of time (9

hours and 10.5 hours), leading to hyperbranched polymers of different sizes, but with the same effective degree of branching. The subscripts at the end of these respective codes differentiate the samples by the measured molecular weight of each polymer according to SEC. Note that the general polymerization time of nine hours was determined to be ideal to ensure that conversion was sufficient while ensuring that the final functionalized product be soluble.

Aqueous SEC,  $^1\text{H-NMR}$ , and conductometric titration analyses were used to characterize each of the polymers, with the results shown in Table 2.2 and Figures S.1 to S.7. The recorded PDI values range between 1.20 (for DoB = 0, or linear polymers prepared) and 2.49 (for the highest branched, largest hyperbranched polymer), with PDI increasing systematically as a function of both the degree of branching as well as the reaction time. A PDI of  $< 1.3$  indicates a controlled polymerization, consistent with the results for both linear polymers and suggesting effective controlled radical polymerization with the polymerization conditions used. However, while the individual polymer chains in the hyperbranched polymers are expected to retain this controlled, living property, the growth of these hyperbranched polymer structures as a whole is not necessarily linear, as per the mechanism illustrated schematically in Figure 2.2. As each hyperbranched molecule grows and branches, the probability of that molecule finding, and thus, reacting with another hyperbranched molecule over a monomer unit increases. Indeed, if the system is left to react for long enough, the result is a bulk hydrogel, based on both continual intramolecular crosslinking during chain growth as well as intermolecular crosslinking mediated by the presence of pendant double bonds from EGDMA units that

are incorporated into the structure but do not form a crosslink/branch. The calculated degrees of branching (from NMR) are all slightly lower than the expected value based on each EGDMA group incorporated being one branch point, confirming the presence of a significant fraction (~3-5 mol% based on the total monomer content) of pendant double bonds in the hyperbranched materials. Therefore, instead of having all molecules of the same size, the final product will consist of a wider distribution of molecular sizes depending on how many other hyperbranched molecules react (and thus effectively aggregate together) as well as the size of those hyperbranched molecules.

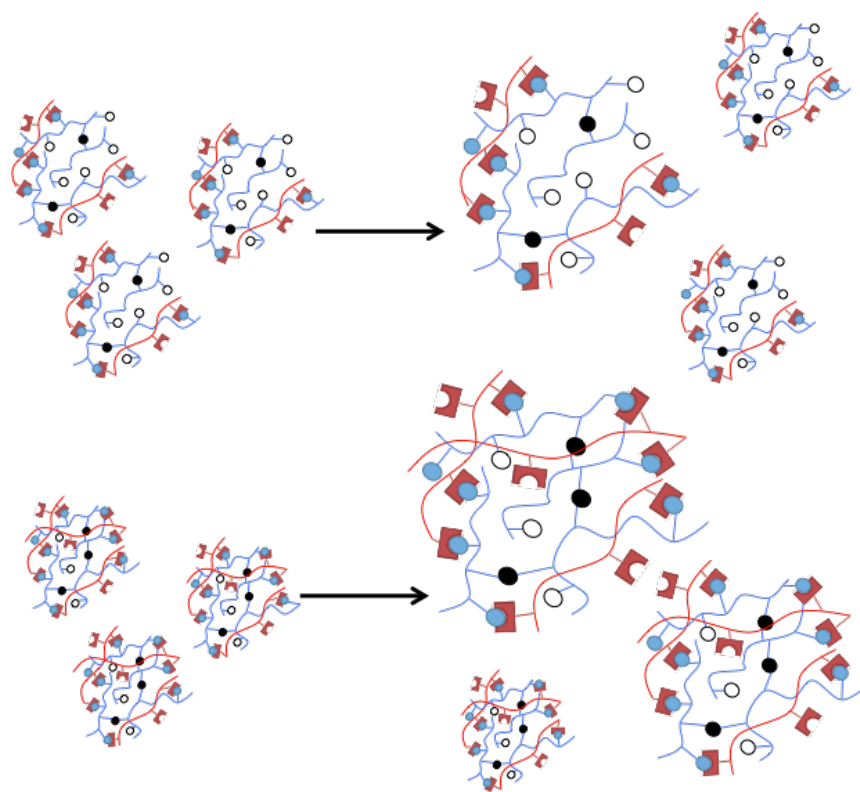


**Figure 2.2.** Scheme for the hypothesized growth mechanism of the hyperbranched polymer precursors. The top image shows growth for less branched molecules, while the bottom depicts growth for more highly branched molecules.

The change in molecular weight, polydispersity, and conversion of each polymer were observed over the course of the 9 hour polymerization reaction time, results for which are shown in Figure S.8 in the Appendix. For the hyperbranched polymers (DoB = 5, 10, and 15%), the final conversion values are all relatively similar, ranging from 81 to 83%. However, for the linear polymer (DoB = 0%), the conversion was slightly lower at ~67%. This observation is likely related to the transfer constant of the CPCBD RAFT agent being lower for OEGMA than EGDMA due to steric hindrance of the side chains of the OEGMA monomer. Consequently, at higher mole fractions of EGDMA, chain transfer and thus, conversion are accelerated. In terms of molecular weight, the absolute molecular weight, the rate of molecular weight increase, the absolute polydispersity, and the rate of change in polydispersity all increased as a function of the degree of branching (Figure S.8B,C). As previously indicated, hyperbranched molecules would grow independently at the start of the polymerization reaction (low conversion), reflected in the data by the nearly constant molecular weight versus time profiles and linear molecular weight versus conversion profiles observed at short reaction times (Figure S.8D). In the absence of EGDMA, the molecular weight versus conversion curve persists as linear and the polydispersity remains unchanged as a function of time, indicative of living controlled free radical polymerization. However, in the presence of EGDMA at higher conversions, the molecular weight versus conversion profile becomes markedly steeper and both the molecular weight and polydispersity sharply increase with reaction time, with higher increases observed at higher DoB values. This result can again be rationalized based on the mechanism of hyperbranched polymer preparation; that is, as the reaction progresses

and monomer concentration decreases, the probability of a branch point forming between two hyperbranched molecules significantly increases, leading to the formation of on average larger and more polydisperse molecules.

Lastly, the degree of MAA functionalization of the hyperbranched polymers and the efficiency of the conversion of MAA groups to hydrazide groups was determined using conductometric titration. Results, shown in Table 2.2, suggest ~50% grafting of MAA groups with hydrazide groups, producing polymers with ~13 to 16 mol% of the total monomer residues containing hydrazide functionality. It should be noted that the efficiency of functionalization does not change as a function of DoB, suggesting that this limitation on grafting is predominantly a function of the chemistry and not steric hindrance. On the other hand, aldehyde functionalization for the linear polymer proceeded to only ~33% conversion, corresponding to 10 mol% of total monomer residues being converted to an aldehyde group. This may be attributed to the lower efficiency of the EDC reaction in the organic solvent used for this functionalization, although non-stoichiometric acetal group deprotection may also contribute to this result based on inconsistencies between NMR end-group analysis and acetal grafting results from titration. In order to drive this reaction to higher conversions, it may be pertinent to add a base to the reaction to neutralize the acidic portion of the EDC structure. None of the hyperbranched or linear polymers exhibited a cloud point in water, consistent with expected results when using POEGMA with higher ( $n = 8-9$ ) numbers of ethylene oxide repeat units in the side chain (Lutz, *Polymer Science*, 2008).

**Table 2.2.** Chemical characteristics of the synthesized hyperbranched and linear POEGMA polymers. All polymers were polymerized for 9 hours except for the HBP<sub>H</sub>15<sub>25</sub> polymer, which was polymerized for 10.5 hours. Composition, functionalization, and DoB values were calculated using NMR and titration data. Molecular weight and PDI values were obtained from aqueous SEC. Cloud point values were > 90°C for all polymers and were determined using UV-vis spectrophotometry.

Polymer	MAA [mol %]	OEGMA [mol %]	EGDMA [mol %]	DoB [%]	Res. Vinyl [mol %]	M <sub>n</sub> x 10 <sup>3</sup> [g/mol]	PDI [-]	Func. [%]
HBP <sub>H</sub> 15 <sub>22</sub>	26.1	56.9	17.0	13.4	3.6	22.1	2.27	13
HBP <sub>H</sub> 15 <sub>25</sub>	26.3	57.9	15.8	12.6	3.2	25.4	2.49	14
HBP <sub>H</sub> 10	28.9	58.1	13.0	9.2	3.8	19.8	1.80	15
HBP <sub>H</sub> 5	25.8	66.7	7.5	4.5	3.0	15.6	1.36	14
HBP <sub>H</sub> 0	29.6	70.4	0	0	N/A	13.9	1.20	16
HBP <sub>A</sub> 15	30.8	47.8	21.4	16.4	5.0	15.5	1.94	16
HBP <sub>A</sub> 0	29.8	70.2	0	0	N/A	14.5	1.22	10

MAA - methacrylic acid; OEGMA - oligo(ethylene glycol) methacrylate; EGDMA - ethylene glycol dimethacrylate; DoB - degree of branching; Res. Vinyl - residual pendant vinyl groups (= [EGDMA] - DoB); M<sub>n</sub> - number average molecular weight; PDI - polydispersity; Func. - degree of functionalization.

Hydrogels were formed by mixing the hydrazide and aldehyde functionalized precursor polymers. Most gels consisted of hydrazide-functionalized hyperbranched polymers mixed with aldehyde-functionalized linear polymers aside from the HBP<sub>H</sub>15<sub>22</sub>/HBP<sub>A</sub>15 (HB-HB15) hydrogel that consisted of a mixture of two hyperbranched polymers, both with the same effective degree of functionalization as the linear polymers (see above). The effective gelation time of each hydrogel (as measured via the vial inversion test) is shown in Table 2.3.

**Table 2.3.** Comparison of gelation time for various hyperbranched-linear and hyperbranched-hyperbranched polymer combinations at 22°C (20 wt% of each reactive polymer).

Hydrogel Composition	Gelation Time [min]
HB15 (HBP <sub>H</sub> 15 <sub>22</sub> + HBP <sub>A</sub> 0)	10
HB10 (HBP <sub>H</sub> 10 + HBP <sub>A</sub> 0)	15
HB5 (HBP <sub>H</sub> 5 + HBP <sub>A</sub> 0)	20
HB0 (HBP <sub>H</sub> 0 + HBP <sub>A</sub> 0)	35
HB15 <sub>High MW</sub> (HBP <sub>H</sub> 15 <sub>25</sub> + HBP <sub>A</sub> 0)	10
HB15 <sub>50wt%</sub> (HBP <sub>H</sub> 15 <sub>22</sub> – 50wt% + HBP <sub>A</sub> 0 – 50wt%)	3
HB-HB15 (HBP <sub>H</sub> 15 <sub>22</sub> + HBP <sub>A</sub> 15)	10

As the degree of branching was decreased, the gelation time increased, with only 10 minutes required for gelation of the DoB = 15% hydrogel, regardless of whether or not the hydrazide hyperbranched polymer was gelled with a linear or hyperbranched aldehyde polymer, while 35 minutes was required for the DoB = 0% hydrogel with the same degree of functionalization. This result is consistent with the hyperbranched precursors essentially being “pre-crosslinked”, requiring fewer new crosslinks between chains to be made to effectively gel the precursor solutions. The relationship between these gelation times and crosslinking was further tested by evaluating the efficiency of crosslinking between hydrazide and aldehyde groups in the hydrogel via fluorescent labelling of residual functional hydrazide residues in each of the hydrogels by hydrazide-reactive FITC. As shown in Figure 2.3, each of the hydrogels exhibit relatively the same amount of residual functional groups, as expected based on the similarity in functionalization of

the polymer precursors and the assumption that the unreacted hydrazide groups would be accompanied by an equal amount of unreacted aldehyde groups. On the other hand, the hyperbranched-hyperbranched hydrogel exhibited a significantly higher quantity of unreacted hydrazide groups, despite the larger total number of aldehyde groups available for crosslinking in this system relative to the hyperbranched-linear hydrogels ( $p < 0.05$ ). This may be attributed to functional group availability being hindered by dense branching within the polymer molecules. Due to the high crosslink density (both permanent and dynamic), the hyperbranched polymers would become stiffer and prevent possible reactive sites from being accessible. The significant loss of mobility (and likely steric accessibility of reactive functional groups) when both the hydrazide and aldehyde reactive precursor polymers are hyperbranched results in significantly lower degrees of crosslinking (i.e. higher residual functional group contents) in this hyperbranched-hyperbranched hydrogel.

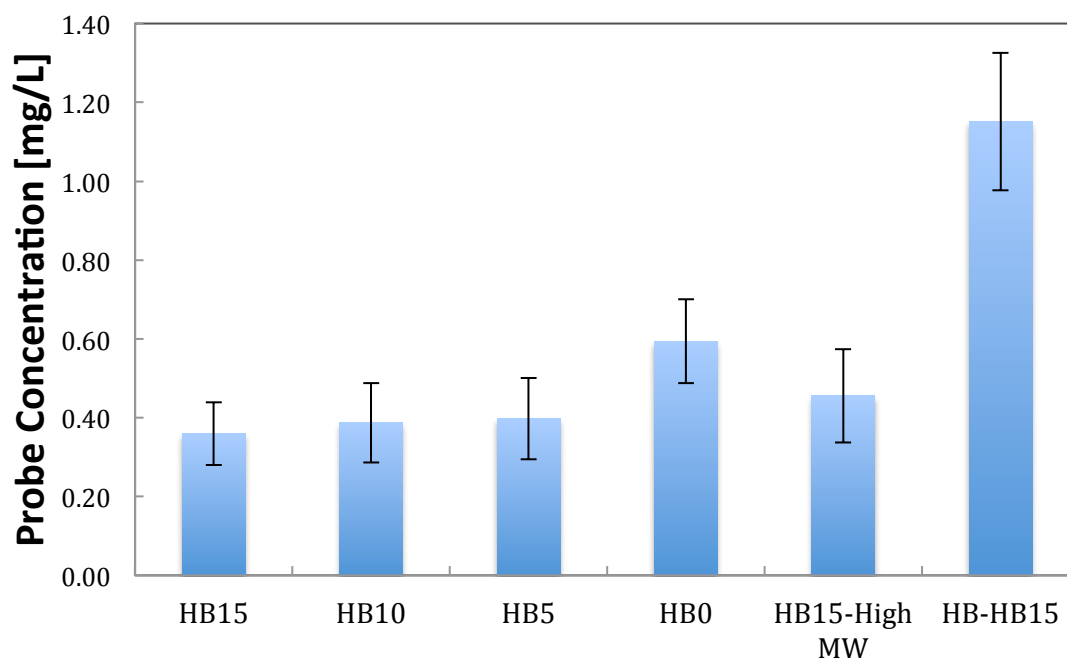


**Figure 2.3.** Measurements of relative fluorescence of hydrazide-reactive FITC bound to unreacted hydrazide functional groups in all hyperbranched-linear and hyperbranched-hyperbranched POEGMA hydrogels. Error bars for each measurement represent one standard deviation value from the mean ( $n = 4$ ).

### 2.3.2. Hydrogel Rheology

The mechanical properties for each hydrogel were tested under both compressive and shear stress. Figure 2.4 shows how the shear storage modulus ( $G'$ ) increases in a non-linear fashion with the DoB. By increasing the DoB, more internally crosslinked, dense, and compact precursor polymers result that lead to hydrogels that are able to withstand higher shear stress, leading to a more than 6-fold increase in the shear modulus of the gel prepared with the same OEGMA monomer and the same degree of hydrazide functionalization.

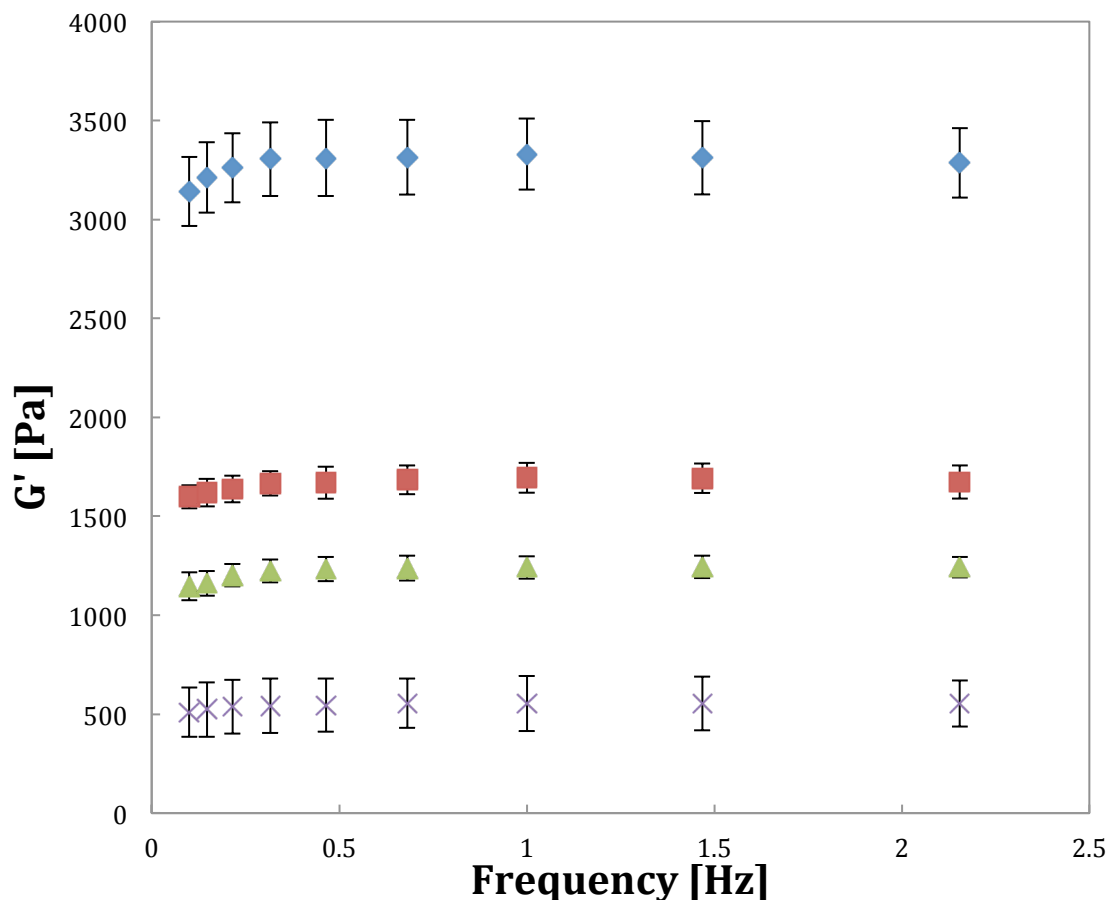


**Figure 2.4.** Mechanical properties of the varying DoB series of hyperbranched POEGMA hydrogels at 22°C. (◆, blue) HB15; (■, red) HB10; (▲, green) HB5; (×, purple) HB0. Error bars for each measurement represents one standard deviation value from the mean ( $n = 3$ ).

However, the absolute shear modulus (while in the range of some soft tissues in the body) is still relatively low, even in the context of *in situ* gelling hydrogels (Levental et al., 2007). In an attempt to get higher  $G'$  values, the molecular weight of the hydrazide-functionalized polymer was increased (HBP<sub>H1525</sub>), the polymer concentrations were increased to 50 wt%, and a hyperbranched aldehyde-functionalized polymer was utilized (HBP<sub>A15</sub>) instead of the linear version. The corresponding rheological data for hydrogels

prepared with these modified precursor polymers is presented in Figure 2.5. When both polymer precursors were hyperbranched (DoB = 15%), the shear modulus decreases significantly, which is consistent with the significantly higher number of residual functional groups (and thus, lower crosslink densities) observed in this gel in the fluorescence assay (Figure 2.3). As hypothesized earlier, this result is most likely due to a combination of increased steric hindrance and reduced polymer flexibility, leading to the formation of fewer crosslinks and resulting in a weaker gel even though the precursor polymers themselves are denser and more internally crosslinked. Increasing the molecular weight of the hydrazide-functionalized polymer precursor resulted in essentially no difference in mechanical strength, indicating that polymer size is not as significant as branching as a determinant for rheological properties (at least on the relatively small size range investigated in this work). However, increasing the concentration of HBP<sub>H1522</sub> and HBP<sub>A0</sub> precursor polymers to 50 wt% did result in a higher G' value, although one that was lower than expected. The significantly faster gelation time of this concentrated mixture (3 minutes versus 10 minutes at 20 wt%) may kinetically arrest the system at lower degrees of crosslinking, limiting the mechanical benefit to be derived from this higher concentration mixture.

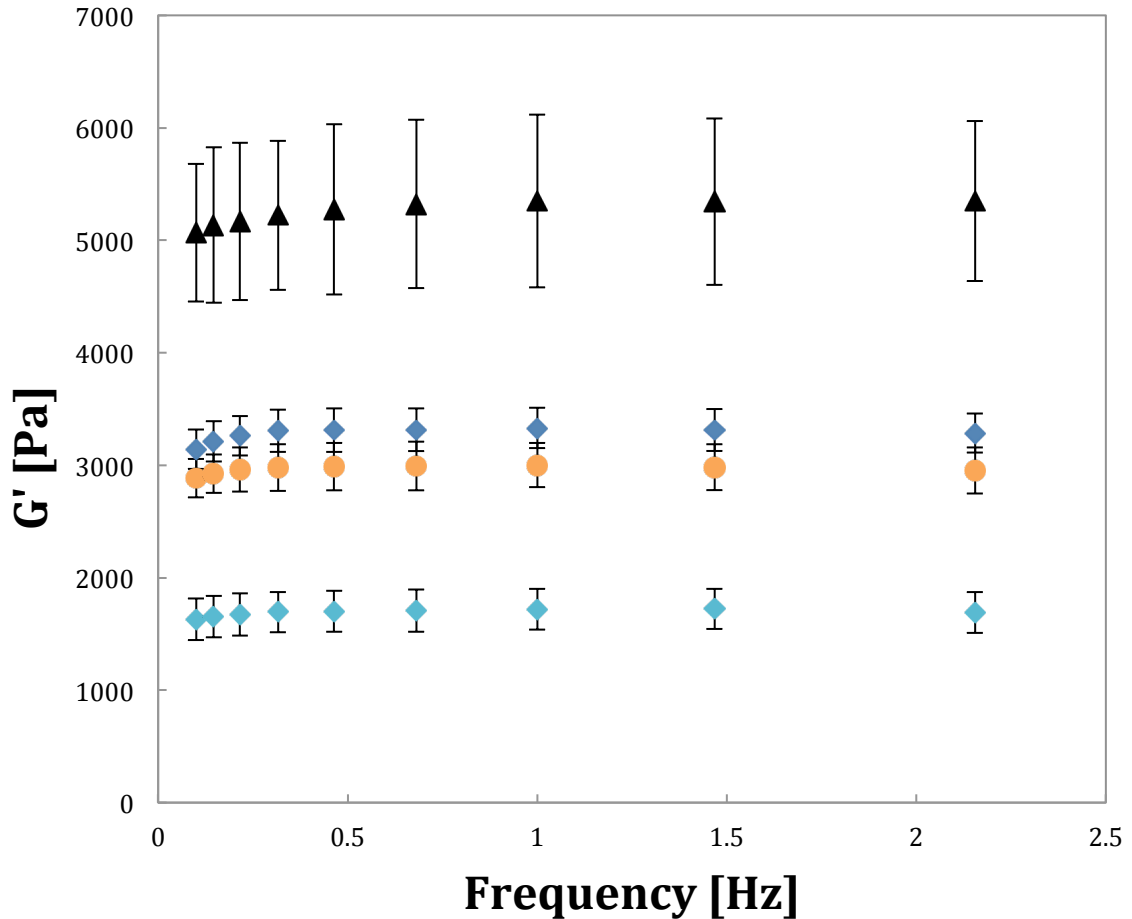


**Figure 2.5.** Mechanical properties of the 15% DoB hyperbranched POEGMA hydrogel series at 22°C. (◆, blue) HB15; (●, orange) HB15<sub>High MW</sub>; (◆, aqua) HB-HB15; (▲, black) HB15<sub>50wt%</sub>. Error bars for each measurement represents one standard deviation value from the mean ( $n = 3$ ).

Table 2.4 compares the shear storage modulus ( $G'$ ), compressive modulus, and transmittance values for each hydrogel tested. As stated previously,  $G'$  generally increases with DoB and increasing precursor solution concentrations, is relatively insensitive to the molecular weight of the hyperbranched polymer precursor, and decreases if both precursor polymers are hyperbranched. The absolute values of the moduli are comparable to other POEGMA hydrogels previously reported (Bakaic,

Dorrington et al., 2015; Smeets, Bakaic et al., 2014). Similarly, the compressive modulus increases in a non-linear manner as a function of DoB, ranging between 7 kPa (DoB = 0%) and 18 kPa (DoB = 15%), is insensitive to the molecular weight of the hyperbranched precursor polymer, and is lower for hyperbranched-hyperbranched gels relative to hyperbranched-linear hydrogels. Interestingly, the higher concentration HB15<sub>50wt%</sub> hydrogel did not show a significantly enhanced compressive modulus despite the significantly higher mass concentration in this hydrogel, a result we attribute to the relatively lower degree of crosslinking in the network due to the faster gelation time, as previously mentioned. It is hypothesized that the faster gelation time results in faster immobilization of the chains and thus a lower potential for achieving similar percentage crosslink formation. The transmittance values for each hydrogel, except for HB-HB15, are relatively the same as the PBS-only reference, suggesting they are all highly transparent. The slight opacity observed in the all-hyperbranched HB-HB15 hydrogel is attributable at least in part to the hyperbranched aldehyde-functionalized polymer precursor solution being somewhat opaque, unlike all other precursors that are transparent. This difference was attributed to issues with polymer precursor solubility as both SEC (molecular weight) and NMR (chemical functionalization) reported expected values of polymer properties (Table 2.2). We anticipate this moderate solubility may be attributable to hemiacetal formation within the aldehyde-functionalized hyperbranched polymer when dissolved in an aqueous solvent, a process that may be accelerated in hyperbranched polymers versus linear polymers given the closer fixed proximity between adjacent aldehyde groups in the hyperbranched polymer (Zhu et al., 2006). Therefore, it is

possible to tune the mechanical strength of these hyperbranched hydrogels without sacrificing transparency, which may be ideal for ophthalmic applications.

**Table 2.4.** Comparison of shear storage modulus, compressive modulus, and transmittance (at 595 nm) for each hyperbranched hydrogel at 22°C. For reference, the same volume of PBS has an average transmittance of 92.0% at 22°C in the measurement plate. Error values for each measurement represents one standard deviation value from the mean ( $n = 3$ ).

Hydrogel Composition	Average Shear Storage Modulus [kPa]	Average Compressive Modulus [kPa]	Transmittance [%]
HB15	3.27 ± 0.18	18.30 ± 2.71	91.7
HB10	1.66 ± 0.07	10.71 ± 1.93	91.2
HB5	1.21 ± 0.06	9.02 ± 0.11	91.2
HB0	0.54 ± 0.13	7.47 ± 1.09	90.9
HB15 <sub>High MW</sub>	2.96 ± 0.20	16.94 ± 0.58	91.5
HB15 <sub>50wt%</sub>	5.25 ± 0.71	12.94 ± 1.20	89.6
HB-HB15	1.69 ± 0.18	9.86 ± 0.50	78.8

### 2.3.3. Swelling and Degradation Kinetics

To determine the swelling ratios and degradation profiles of each hyperbranched POEGMA hydrogel, gravimetric assays were performed in 10 mM PBS and 10 mM HCl (acid-catalyzed conditions) at physiological temperature (37°C). Swelling profiles were also assessed at room temperature (about 22°C) for further characterization over a longer period of time, the results of which are shown in Figures S.9 and S.10 in the Appendix. To make analysis easier, results were broken down into two separate series – hyperbranched-linear gels prepared with hydrazide-functionalized hyperbranched

polymers with varying degrees of branching (DoB = 0 to 15%) and the series of modified hydrogels with DoB = 15% (HB15, HB15<sub>High MW</sub>, and HB-HB15).

Figures 2.6 and 2.7 show the degradation profiles under acid-catalyzed conditions at physiological temperature. Each hydrogel exhibits a similar profile consisting of some initial swelling followed by rapid degradation, leading to complete gel-sol transition within one day. The kinetic profiles observed are consistent with a diffusion-limited degradation – as bonds are hydrolytically cleaved, more acid is able to penetrate the hydrogel network, accelerating the degradation process. Figure 2.6 shows that the degradation rate is inversely correlated with the DoB – hydrogels prepared with more hyperbranched polymers degrade more slowly. With less internal crosslinking in the precursor polymers (lower DoB), the hydrogel is able to take on more water more quickly, exposing more bonds to be hydrolytically cleaved and effectively decreasing the time for degradation. This result represents an advantage of using hyperbranched precursor polymers for gel formation, as longer stability can be achieved while only slightly changing the net chemical composition of the hydrogel. This effect is accentuated at lower pH, as the polymers collapse even further due to protonation of the residual –COOH groups on the hydrazide-functionalized polymer, thus limiting the accessibility of acid to crosslink sites. In the case of HB15<sub>High MW</sub>, the increase in polymer precursor size with the same degree of functionalization may cause fewer reactive functional groups to be available at the interface of the polymer molecules, thus allowing relatively fewer crosslinks to form, making it easier to be degraded more quickly. The HB-HB15 hydrogel degrades faster than HB15, consistent with the fluorescent probe results that indicate

lower effective consumption of reactive functional groups due to the less flexible nature of the building block polymer.

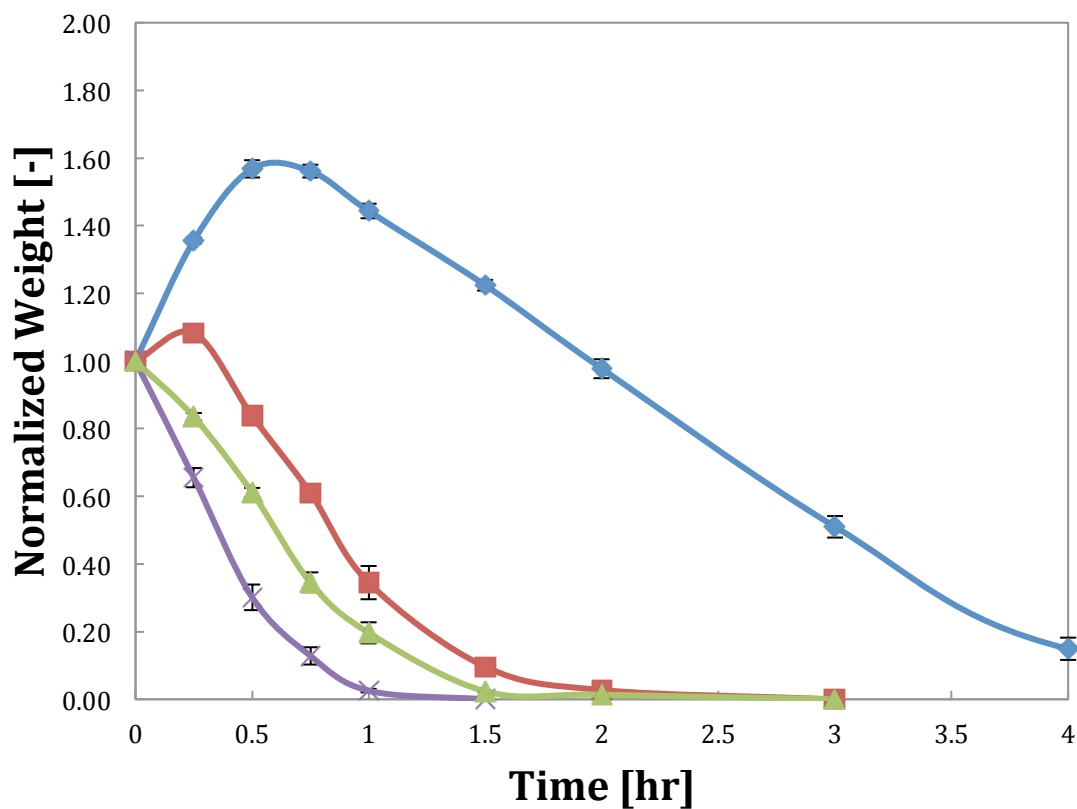


**Figure 2.6.** Degradation kinetics of the varying DoB series of hyperbranched POEGMA hydrogels in 10 mM HCl at 37°C. (♦, blue) HB15; (■, red) HB10; (▲, green) HB5; (×, purple) HB0. Error bars for each measurement represents one standard deviation value from the mean ( $n = 3$ ).

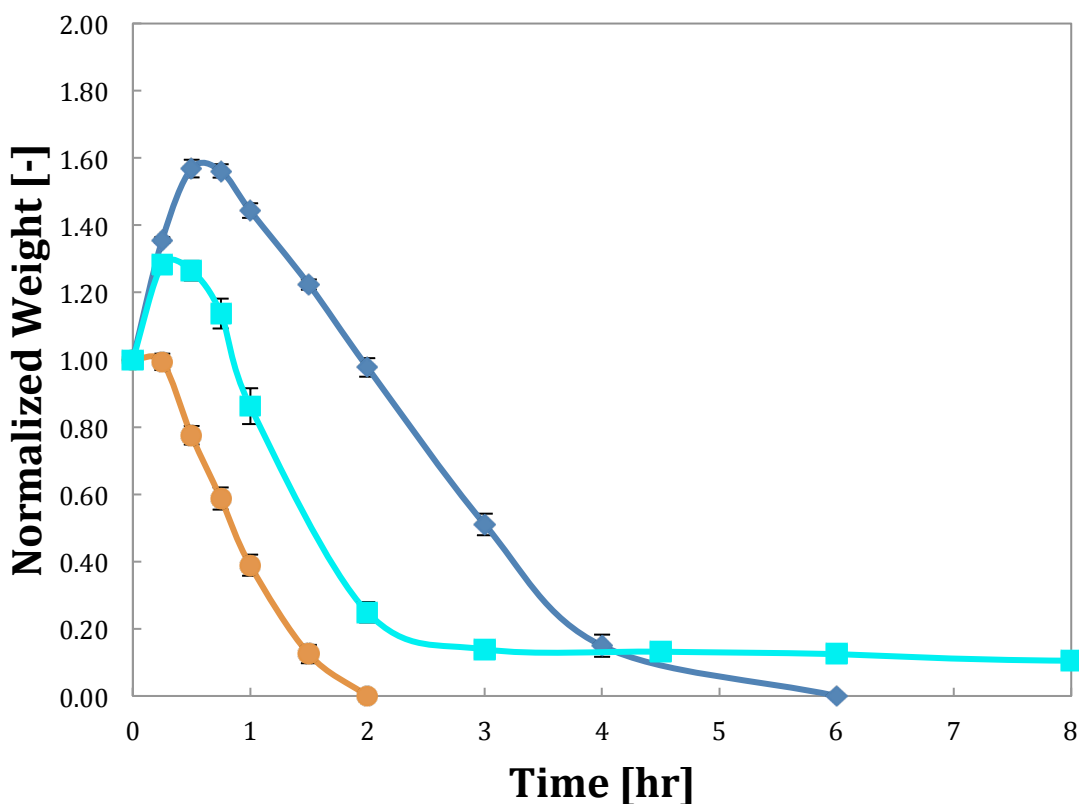


**Figure 2.7.** Degradation kinetics of the 15% DoB hyperbranched POEGMA hydrogel series in 10mM HCl at 37°C. (◆, blue) HB15; (●, orange) HB15<sub>High MW</sub>; (■, aqua) HB-HB15. Error bars for each measurement represents one standard deviation value from the mean ( $n = 3$ ).

Figures 2.8 and 2.9 depict the swelling profiles for both hydrogel series in PBS at physiological temperature (37°C). First, while the profiles generally mirror the trends seen in the degradation assays, the hydrogels swelled significantly more in PBS than in HCl, attributable to deprotonation of the residual carboxyl groups (not functionalized with hydrazide or aldehyde groups) on the precursor polymers at a neutral pH that drives Donnan equilibrium-based swelling responses. Moreover, it is again confirmed that the degradation time of the hydrogel increases with the degree of branching within the

polymer precursor due to the higher number of hydrazone bonds that need to be hydrolytically cleaved before the network can be completely degraded. Interestingly, the hyperbranched-hyperbranched hydrogel exhibits a plateau at a significantly lower degree of swelling after the initial swell and degrades much more slowly (over 200 hours versus <100 hours for each of the linear-linear or hyperbranched-linear hydrogels studied) despite containing fewer hydrazone linkages that hold the bulk gel together (Figure 2.3). However, when comparing the time scales for the degradation vs. swelling assays, it should be noted that since these hydrogels are made in PBS, degradation in acidic conditions would be dependent on the diffusion of HCl into the system, whereas in a PBS environment the system is already at an equilibrium and would take longer to degrade overall. On the other hand, we hypothesize that the observations for the hyperbranched-hyperbranched hydrogel are related to the hyperbranched structure of the precursor polymers, in which fixed, hydrolytically stable crosslinks are already formed in the starting components. In this context, there is significantly less potential for swelling given the higher net crosslink density in the gel when combining both the hydrazone linkages between hyperbranched polymers and the crosslinks within each hyperbranched polymer. Similarly, a higher percentage of the even smaller number of hydrazone crosslinks formed likely need to degrade to functionally convert the hyperbranched-hyperbranched network back to a sol state given that a large fraction of the overall crosslinks present in the system are non-degradable in the conditions used for this test. Similar trends were noted at 22°C, although the times required for total degradation times were roughly 3-fold longer than observed at 37°C, consistent with conventional Arrhenius-like temperature

dependence on hydrolysis rate constants (see Appendix Figures S.9 and S.10). Collectively, these results again clearly show the potential benefits of using hyperbranched polymers as hydrogel precursor polymers to effect differences in gel properties (in this case, substantially reducing the magnitude of swelling and extending the gel degradation time) without substantially changing gel chemical compositions.

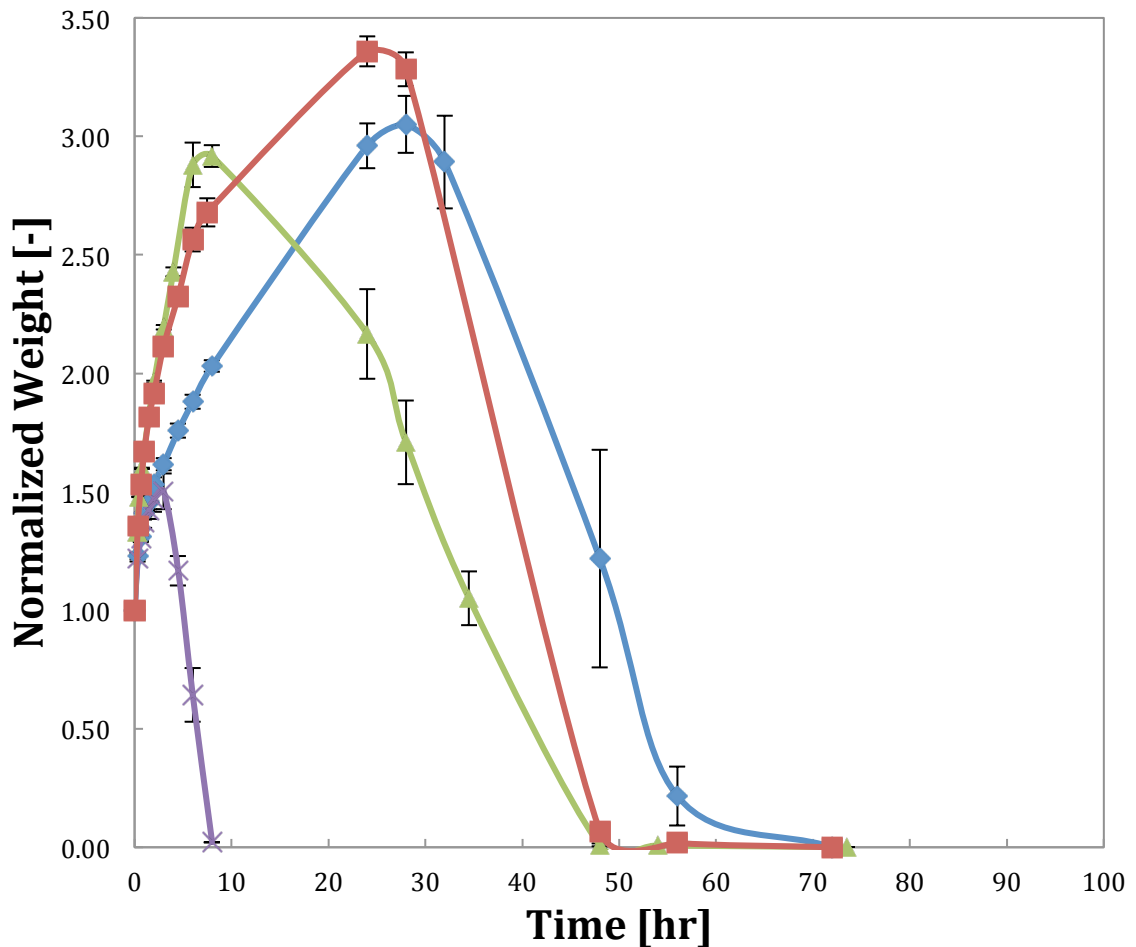


**Figure 2.8.** Swelling kinetics of the varying DoB series of hyperbranched POEGMA hydrogels in 10mM PBS at 37°C. (♦, blue) HB15; (■, red) HB10; (▲, green) HB5; (×, purple) HB0. Error bars for each measurement represents one standard deviation value from the mean ( $n = 3$ ).

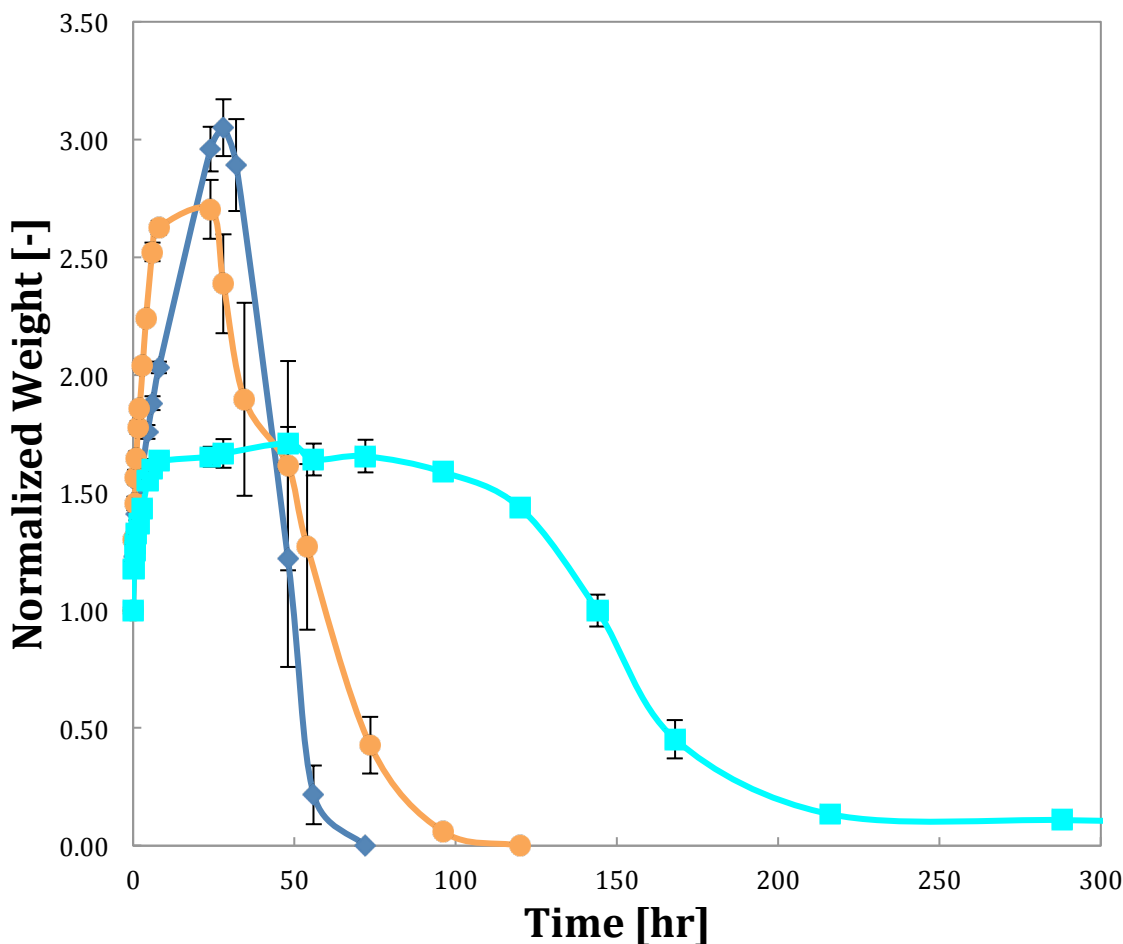


**Figure 2.9.** Swelling kinetics of the 15% DoB hyperbranched POEGMA hydrogel series in 10mM PBS at 37°C. (◆, blue) HB15; (●, orange) HB15<sub>High MW</sub>; (■, aqua) HB-HB15. Error bars for each measurement represents one standard deviation value from the mean ( $n = 3$ ).

### 2.3.4. Cytotoxicity of Polymer Precursors

The cytotoxicity of all hyperbranched polymers was determined using a resazurin assay with 3T3 mouse fibroblasts. As shown in Figure 2.10, most polymers did not exhibit significant cytotoxicity, even at concentrations (2 mg/mL) that are relatively high for testing in closed *in vitro* assay systems (Smeets, Bakaic et al., 2014). It should be noted that the HBP<sub>H</sub>15<sub>25</sub> and HBP<sub>A</sub>15 polymers appeared to be slightly more cytotoxic at

some concentrations. This decrease in viability may be attributed to the assay for these two precursors being performed at a different time, by a different person, and with a different cell culture (the initial state of which was not ideal) despite the assay conditions being maintained.

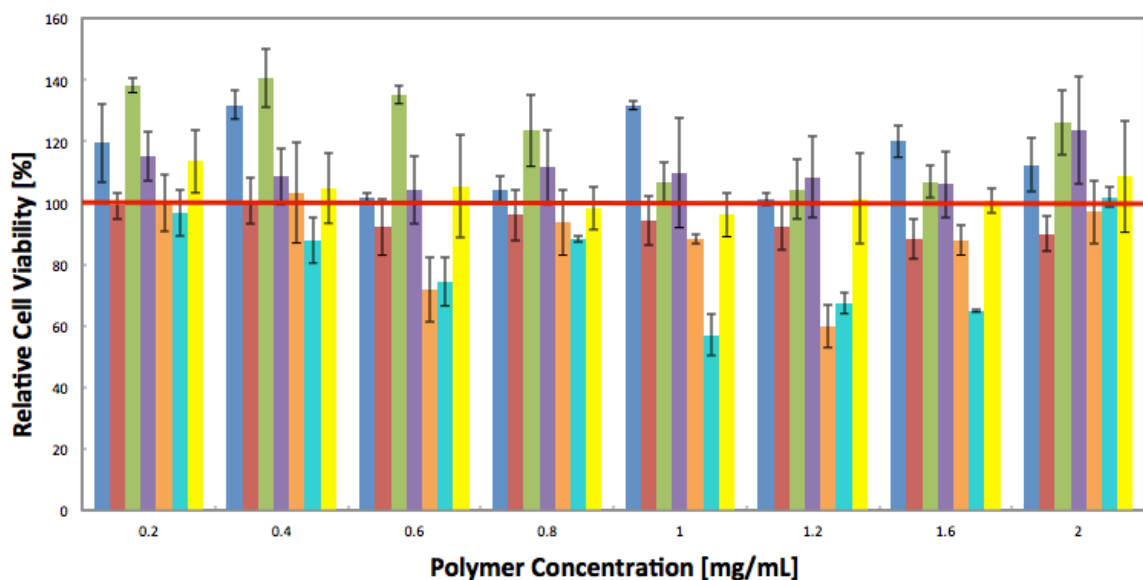


**Figure 2.10.** Relative viability of 3T3 mouse fibroblasts treated with HBP<sub>H</sub>15<sub>22</sub> (blue), HBP<sub>H</sub>10 (red), HBP<sub>H</sub>5 (green), HBP<sub>H</sub>0 (purple), HBP<sub>H</sub>15<sub>25</sub> (orange), HBP<sub>A</sub>15 (aqua), and HBP<sub>A</sub>0 (yellow) for 24 hours at concentrations ranging from 0.2 to 2 mg/mL. Error bars for each measurement represents one standard deviation value from the mean of measured percent cell viability ( $n = 4$ ).

### 2.3.5. Protein Adsorption

Protein adsorption of all hyperbranched hydrogels was determined by exposing the hydrogels to fluorescently labelled BSA, thoroughly rinsing the hydrogels to remove any unadsorbed protein, and measuring relative fluorescence. As shown in Figure 2.11, in general, introducing hyperbranched polymers into the hydrogels slightly increases the concentration of adsorbed protein to hydrogels, with statistically significant increases in

protein adsorption noted between most hyperbranched-linear hydrogel and the hyperbranched-hyperbranched system ( $p < 0.05$ ). Correspondingly, the hyperbranched-hyperbranched hydrogel almost always adsorbed the most BSA among all the tested gels, consistent with the hyperbranched polymer content being effectively doubled in this gel (although the higher residual functional group content in this hydrogel (Figure 2.3) may also contribute to this result). However, the trend with the DoB is not linear, with protein adsorption increasing from DoB = 0 to DoB = 10 but then significantly decreasing at DoB = 15, a result that was consistent for both the smaller and larger DoB = 15 gels. The reason for this trend is not immediately clear and will be the subject of further investigation to determine if protein interactions with residual aldehyde groups are causing more protein to be adsorbed or if any protein is being absorbed into the hydrogel mesh. However, these results suggest promise in terms of enabling the preparation of gels that exploit the key advantages of the hyperbranched structure (i.e. slower degradation, stronger mechanics) without negatively influencing potential biological properties. However, it is important to note that for the two lower concentrations tested, the amount of adsorbed protein remained in the 10 to 100 ng/cm<sup>2</sup> range for similar loading concentrations that has been previously reported for PEG-grafted surfaces (Hou et al., 2010; Unsworth et al., 2005; Du et al., 1997). Even at BSA concentrations of 0.5 mg/mL, the maximum adsorption amount of 217 ng/cm<sup>2</sup> was still significantly lower than many other reported polymeric biomaterials (Roach et al., 2006; Tanaka et al., 2000).

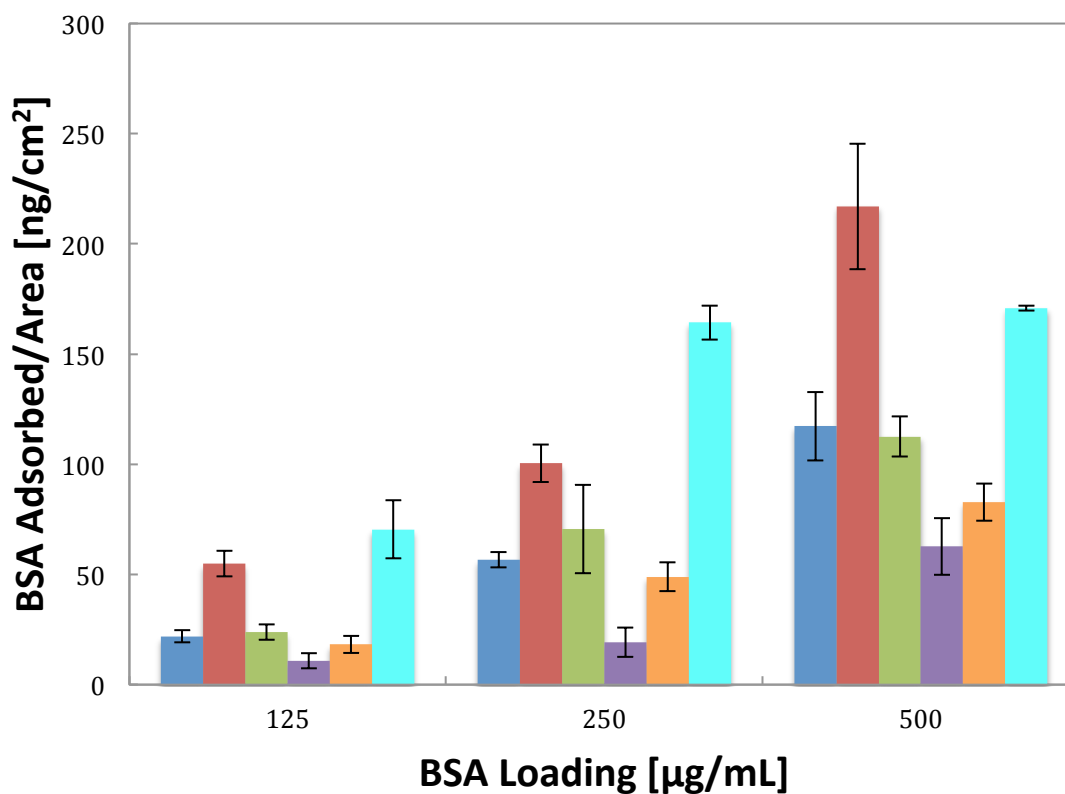


**Figure 2.11.** Adsorption of BSA to hyperbranched POEGMA hydrogels. HB15 (blue), HB10 (red), HB5 (green), and HB0 (purple), HB15<sub>High MW</sub> (orange), HB-HB15 (aqua). Error bars for each measurement represents one standard deviation value from the mean ( $n = 4$ ).

### **Chapter 3 – Conclusions and Future Directions**

A series of hyperbranched POEGMA polymers was successfully synthesized using RAFT polymerization. Based on chemical characterization, these polymers were similar except for the crosslinking density or degree of branching (DoB). Using NMR analysis, it was determined that the actual DoB values for each polymer were close to the targeted values of 0, 5, 10, and 15%. Furthermore, the molecular weight, conversion, and dispersity all positively correlated with the amount of crosslinker incorporated into the polymer network. Functionalization of the polymers with hydrazide and aldehyde groups proceeded to 50-60% and 33% conversion, respectively, of acrylic acid residues based on conductometric titration, with the observed grafting efficiency being independent of polymer precursor composition.

Subsequently, a series of hyperbranched-linear and hyperbranched-hyperbranched hydrogels was successfully produced. The mechanical properties of these hydrogels exhibited a positive correlation between degree of branching and shear storage modulus. Moreover, the hyperbranched-hyperbranched system exhibited reduced mechanical strength and shear modulus relative to the hyperbranched-linear networks, a result attributed to the relatively lower crosslink density of this hydrogel offsetting the benefits of a more compact polymer structure. Degradation rates under acid-catalyzed conditions as well as swelling rates in PBS tended to decrease with increasing DoB, with the hydrogels swelling to a significantly greater degree in PBS. It is hypothesized that the swelling and degradation profiles are characterized by a balance between polymer size

(steric hindrance) and relative crosslinking density (functional group or reactive site availability). Interestingly, despite the lower effective crosslink density and weaker mechanics of the hyperbranched-hyperbranched hydrogel relative to hyperbranched-linear hydrogels, the hyperbranched-hyperbranched hydrogel showed significantly lower maximum swelling ratios and longer degradation times in comparison to the hyperbranched-linear hydrogels with the same DoB. This is attributed to the effective non-degradability of the majority of the crosslinks in the network (the hyperbranching points) under the conditions studied. Based on a resazurin assay with 3T3 mouse fibroblasts, each of the polymer precursors showed minimal cytotoxicity. Lastly, while the hyperbranched hydrogels adsorbed slightly more protein than other PEG-based hydrogels, they still adsorb significantly less protein in comparison to other polymeric biomaterials, particularly at higher degrees of branching and for all-hyperbranched hydrogels. Overall, we have demonstrated that it is possible to tune the hydrogel properties by altering the structural architecture of the polymer precursors. This would provide another platform for modular hydrogel design, whereby mixing different functional precursor polymers with well-defined properties can systematically alter hydrogel properties.

In order to expand on the knowledge gained from this project, efforts should be made to improve the synthesis of specifically targeted hyperbranched structures to allow for better and more thorough characterization of the chemical properties as well as the physical polymer structure. This may be done by further and more in depth NMR analysis and the incorporation of other analysis techniques such as triple-detection SEC and small

angle neutron scattering (SANS) to gain an understanding of the true molecular weight and internal structure of the polymers, respectively. Furthermore, to specifically confirm the results from the protein adsorption assay performed for this thesis, it may be appropriate to utilize a blocking assay to consume available aldehyde groups to determine whether increases in protein adsorption is attributable to residual aldehyde functional groups. It may also be permissible to use confocal microscopy to determine if and how much protein is being absorbed into the hydrogel network instead of solely adsorbing to the hydrogel surface. Future work may also include optimizing polymer and hydrogel composition to improve the predictability of the physical properties between polymer batches. However, considering there are multiple factors involved in determining these characteristics, optimization may prove to be quite difficult. Along these lines, it would be ideal to develop a more reliable synthesis method with improved functional group grafting efficiency for the hyperbranched and linear aldehyde polymer precursors. By delving further into the literature, it may be possible to determine a functionalization method that is more suited to our POEGMA system and overcomes issues of solubility and reproducibility. Once this has been accomplished, it would be interesting to synthesize a series of aldehyde-functionalized hyperbranched polymers with varying DoB that can be mixed with the hydrazide-functionalized hyperbranched series presented here to form a wider array of hyperbranched-hyperbranched hydrogel networks. This would allow for further insight into how the hyperbranched architecture of both polymer precursors affects the overall hydrogel properties. Moreover, to extend on the 15% DoB polymer precursor modifications, further testing (i.e. swelling, degradation, protein

adsorption, etc.) of the hydrogel with high polymer content (50 wt%) may be conducted. The effects of this could be explored even further by creating yet another series of hydrogels with varying polymer concentrations (i.e. 15, 20, 30, 40, and 50 wt%). Finally, it may be interesting to synthesize a similar series of hyperbranched POEGMA polymers using a monomer with a shorter ethylene glycol side chain, like M(EO)<sub>2</sub>MA, and/or a defined ratio of both OEGMA and M(EO)<sub>2</sub>MA. By incorporating a monomer with a lower LCST, a thermoresponsive element could be introduced into the hydrogels, which may give rise to vastly different mechanical, swelling, and degradation properties (as per previous work with linear precursors of similar compositions) in addition to introducing temperature-responsive components.

Overall, it has been shown that it is possible to significantly tune the physicochemical properties of POEGMA hydrogels by only slight variations in the architecture of the polymer precursors. While the effects of hyperbranching still need to be optimized, this has furthered our knowledge towards the creation of a versatile and tunable platform for hydrogel design, getting us closer to customized treatment and away from the concept of a “one size fits all” biomaterial.

### References

- Abbasi, E., Aval, S., Akbarzadeh, A., Milani, M., et al. *Nanoscale Research Letters* **2014**, *9*.
- Alfurhood, J.A., Sun, H., Bachler, P.R., & Sumerlin, B.S. *Polymer Chemistry – UK* **2016**, *7*, 2099-2104.
- Ardana, A., Whittaker, A.K., & Thurecht, K.J. *Macromolecules* **2014**, *47*, 5211-5219.
- Aziz, M.A., Cabral, J.D., Brooks, H.J.L., McConnell, M.A., et al. *Journal of Biomedical Materials Research Part B: Applied Biomaterials* **2015**, *103*, 332.
- Bakaic, E., Smeets, N.M., Dorrington, H., & Hoare, T. *RSC Advances* **2015**, *5*(42), 33364-33376.
- Bakaic, E., Smeets, N. M., & Hoare, T. *RSC Advances* **2015**, *5*, 35469-35486.
- Beena, M.S., Chandy, T., & Sharma, C.P. *Artificial Cells, Blood Substitutes, and Biotechnology* **1995**, *23*, 175-192.
- Bernstein, R.E., Cruz, C.A., Paul, D.R., & Barlow, J.W. *Macromolecules* **1977**, *10*, 681-686.
- Bhattacharai, N., Ramay, H.R., Gunn, J., Matsen, F.A., et al. *Journal of Controlled Release* **2005**, *103*, 609-624.
- Chanda M. *Boca Raton: CRC Press, Taylor & Francis Group* **2013**.
- Chen, S., Zhang, X.Z., Cheng, S.X., Zhuo, R.X., et al. *Biomacromolecules* **2008**, *9*, 2578-2585.
- Chen, P. *Colloids and Surfaces A: Physicochemical and Engineering Aspects* **2005**, *261*, 3-24.
- Chen, P.C., Kohane, D.S., Park, Y.J., Bartlett, R.H., et al. *Journal of Biomedical Materials Research Part A* **2004**, *70*, 459-466.

Chiefari, J., Chong, Y.K., Ercole, F., Krstina, J., et al. *Macromolecules* **1998**, *31*, 5559-5562.

Chin, S.M., He, H., Konkolewicz, D., & Matyjaszewski, K. *Journal of Polymer Science Part A: Polymer Chemistry* **2014**, *52*, 2548-2555.

Choi, B., Loh, X.J., Tan, A., Loh, C.K., et al. *In-Situ Gelling Polymers* **2015**, 5-35.

Corneillie, S. & Smet, M. *Polymer Chemistry* **2015**, *6*, 850-867.

Cowie, J.M.G & Arrighi, V. *Polymers: Chemistry and Physics of Modern Materials* **2008**, *3*.

Deng, S., Wang, R., Xu, H., Jiang, X., et al. *Journal of Materials Chemistry* **2012**, *22*, 10055-10061.

Desai, P.N., Yuan, Q., & Yang, H. *Biomacromolecules* **2010**, *11*, 666-673.

Dienstknecht, T., Ehehalt, K., Jenei-Lanzl, Z., Zellner, J., et al. *Bull Exp Biol Med* **2010**, *9*, 150-157.

Dong, Y., Gunning, P., Cao, H., Mathew, A., et al. *Polymer Chemistry* **2010**, *1*, 827-830.

Dong, Y., Qin, Y., Dubaa, M., Killion, J., et al. *Polymer Chemistry – UK* **2015**, *6*, 6182-6192.

Dong, Y., Saeed, A., Hassan, W., Keigher, C., et al. *Macromolecules Rapid Communications* **2012**, *33*, 120-126.

Du, H., Chandaroy, P., & Hui, S.W. *Biochimica et Biophysica Acta (BBA)-Biomembranes* **1997**, *1326*, 236-248.

England, R.M. & Rimmer, S. *Polymer Chemistry* **2010**, *1*, 1533-1544.

Esfand, R. & Tomalia, D.A. *Dendrimers and other dendritic polymers* **2001**, 587-604.

Fu, H., Cheng, S., Zhang, X., & Zhuo, R. *Journal of Gene Medicine* **2008**, *10*, 1334-1342.

M.A.Sc. Thesis – H. Dorrington; McMaster University – Chemical Engineering

Gaharwar, A.K., Peppas, N.A., & Khademhosseini, A. *Biotechnology and bioengineering* **2014**, *111*, 441-453.

Gao, C. & Yan, D. *Progress in Polymer Science* **2004**, *29*, 183-275.

Gunatillake, P.A., Odian, G., & Tomalia, D.A. *Macromolecules* **1988**, *21*, 1556-1562.

Gupta, D., Tator, C.H., & Shoichet, M.S. *Biomaterials* **2006**, *27*, 2370-2379.

Hadjichristidis, N., Pitsikalis, M., Pispas, S., & Iatrou, H. *Chemical reviews* **2001**, *101*, 3747-3792.

Hassan, W., Dong, Y., & Wang, W. *Stem Cell Research Therapy* **2013**, *4*.

Heskins, M. & Guillet, J.E. *Journal of Macromolecular Science—Chemistry* **1968**, *2*, 1441-1455.

Hoare, T.R. & Kohane, D.S. *Polymer* **2008**, *49*, 1993-2007.

Hou, Y., Schoener, C.A., Regan, K.R., Munoz-Pinto, D., et al. *Biomacromolecules* **2010**, *11*, 648-656.

Isaure, F., Cormack, P., & Sherrington, D.C. *Macromolecules* **2004**, *37*, 2096-2105.

Ishizu, K., Ohta, Y., & Kawauchi, S. *Macromolecules* **2002**, *35*, 3781-3784.

Jia, Z., Chen, H., Zhu, X., & Yan, D. *Journal of the American Chemical Society* **2006**, *128*, 8144-8145.

Jin, H.B., Huang, W., Zhu, X.Y., Zhou, Y.F., et al. *Chemical Society Reviews* **2012**, *41*, 5986-5997.

Jin, R., Hiemstra, C., Zhong, Z., & Feijen, J. *Biomaterials* **2007**, *28*, 2791-2800.

Joshi, N. & Grinstaff, M. *Current Topics in Medicinal Chemistry* **2008**, *8*, 1225-1236.

M.A.Sc. Thesis – H. Dorrington; McMaster University – Chemical Engineering

Kainthan, R.K., Gnanamani, M., Ganguli, M., Ghosh, T., et al. *Biomaterials* **2006**, *27*, 5377-5390.

Kainthan, R.K., Hester, S.R., Levin, E., Devine, D.V., et al. *Biomaterials* **2007**, *28*, 4581-4590.

Kennedy, R., Hassan, W., Tochwin, A., Zhao, T.Y., et al. *Polymer Chemistry – UK* **2014**, *5*, 1838-1842.

Khademhosseini, A. & Langer, R. *Biomaterials* **2007**, *28*, 5087-5092.

Klouda, L. & Mikos, A.G. *European Journal of Pharmaceutics and Biopharmaceutics* **2008**, *6*, 34-45.

Koehler, K. C., Anseth, K. S., & Bowman, C. N. *Biomacromolecules* **2013**, *14*, 538-547.

Kojima, C., Turkbey, B., Ogawa, M., Bernardo, M., et al. *Nanomedicine & Nanotechnology* **2011**, *7*, 1001-1008.

Levental, I., Georges, P.C., & Janmey, P.A. *Soft Matter* **2007**, *3*, 299-306.

Li, J., Harada, A., & Kamachi, M. *Polymer journal* **1994**, *26*, 1019-1026.

Lin, C.C. & Anseth, K.S. *Pharmaceutical Research* **2009**, *26*, 631-643.

Liu, H., Chen, Y., & Shen, Z. *Journal of Polymer Science Part A: Polymer Chemistry* **2007**, *45*, 1177-1184.

Liu, J., Huang, W., Zhou, Y., & Yan, D. *Macromolecules* **2009**, *42*, 4394-4399.

Liu, B., Kazlauciusas, A., Guthrie, J.T., & Perrier, S. *Macromolecules* **2005**, *38*, 2131-2136.

Liu, B., Kazlauciusas, A., Guthrie, J.T., & Perrier, S. *Polymer* **2005**, *46*, 6293-6299.

Liu, L., Namikoshi, T., Zang, Y., Aoki, T., et al. *Journal of the American Chemical Society* **2013**, *135*, 602-605.

M.A.Sc. Thesis – H. Dorrington; McMaster University – Chemical Engineering

Lui, Y.H., Zhang, F.H., & Ru, Y.Y. *Carbohydrate Polymers* **2015**, *117*, 304-311.

Lutz, J. F. *Advanced Materials* **2011**, *23*, 2237-2243.

Lutz, J.F. *Journal of Polymer Science Part A: Polymer Chemistry* **2008**, *46*, 3459-3470.

Lutz, J. F. *Angewandte Chemie International Edition* **2008**, *47*, 2182-2184.

Lutz, J.F., Akdemir, Ö., & Hoth, A. *Polymeric Materials: Science & Engineering* **2006**, *51*, 1052.

Lutz, J. F., & Hoth, A. *Macromolecules* **2006**, *39*, 893-896.

Luzon, M., Boyer, C., Peinado, C., Corrales, T., et al. *Journal of Polymer Science Part A: Polymer Chemistry* **2010**, *48*(13), 2783-2792.

Mateen, R. & Hoare, T. *Journal of Materials Chemistry B* **2014**, *2*, 5157.

Matyjaszewski, K. & Xia, J. *Chemical reviews* **2001**, *101*, 2921-2990.

Mintzer, M.A. & Grinstaff, M. *Chemical Society Reviews* **2011**, *40*, 173-190.

Moad, G., Chong, Y.K., Postma, A., Rizzardo, E., et al. *Polymers* **2004**, *46*, 8458–8468.

Nicodemus, G.D. & Bryant, S.J. *Tissue Engineering Part B: Reviews* **2008**, *14*, 149-165.

O'Brien, N., McKee, A., Sherrington, D.C., Slark, A.T., et al. *Polymer* **2000**, *41*, 6027-6031.

Ornelas, C., Broichhagen, J., & Weck, M. *Journal of the American Chemical Society* **2010**, *132*, 3923-3931.

Oudshoorn, M.H., Penterman, R., Rissmann, R., Bouwstra, J.A., et al. *Langmuir* **2007**, *23*, 11819-11825.

Oudshoorn, M.H., Rissmann, R., Bouwstra, J.A., & Hennink, W.E. *Biomaterials* **2006**, *27*, 5471-5479.

Patenaude, M., Smeets, N., & Hoare, T. *Macromolecular rapid communications* **2014**, *35*, 598-617.

Peppas, N.A., Keys, K.B., Torres-Lugo, M., & Lowman, A.M. *Journal of Controlled Release* **1999**, *62*, 81-87.

Place, E. S., George, J. H., Williams, C. K., & Stevens, M. M. *Chemical Society Reviews* **2009**, *38*, 1139-1151.

Purcell, B.P., Lobb, D., Charati, M.B., Dorsey, S.M., et al. *Nature materials* **2014**, *13*, 653-661.

Rami, L., Malaise, S., Delmond, S., Fricain, J.C., et al. *Journal of Biomedical Materials Research Part A* **2014**, *102*, 3666.

Roach, P., Farrar, D., & Perry, C. *Journal of the American Chemical Society* **2006**, *128*, 3939-3945.

Shi, X., Zhao, Y., Gao, H., Zhang, L., et al. *Macromolecular rapid communications* **2012**, *33*, 374-379.

Smeets, N.M., Bakaic, E., Patenaude, M., & Hoare, T. *Acta Biomaterialia* **2014**, *10*, 4143-4155.

Smeets, N.M., Patenaude, M., Kinio, D., Yavitt, F.M., et al. *Polymer Chemistry* **2014**, *5*, 6811-6823.

Sun, H., Kabb, C.P., & Sumerlin, B.S. *Chemical Science* **2014**, *5*, 4646-4655.

Svenson, S. *Chemical Society Reviews* **2015**, *44*, 4131-4144.

Tai, H., Tochwin, A., El-Betany, A., & Wang, W. *Tissue Engineering Part A* **2015**, *21*, S54-S.

Tai, H., Tochwin, A., & Wang, W. *Journal of Polymer Science Part A: Polymer Chemistry* **2013**, *51*, 3751-3761.

M.A.Sc. Thesis – H. Dorrington; McMaster University – Chemical Engineering

Tanaka, M., Motomura, T., Kawada, M., Anzai, T., et al. *Biomaterials* **2000**, *21*, 1471-1481.

Tian, H., Tang, Z., Zhuang, X., Chen, X., et al. *Progress in Polymer Science* **2012**, *37*, 237-280.

Tomalia, D. & Frechet, J. *Journal of Polymer Science Part A: Polymer Chemistry* **2002**, *40*, 2719-2728.

Tsuji, H. *Macromolecular Bioscience* **2005**, *5*, 569-597.

Unsworth, L.D., Sheardown, H., & Brash, J.L. *Langmuir* **2005**, *21*, 1036-1041.

Van Tomme, S., Storm, G., & Hennink, W. *International journal of pharmaceutics* **2008**, *355*, 1-18.

Van Tomme, S., Van Steenberghe, M., De Smedt, S., Van Nostrum, C., et al. *Biomaterials* **2005**, *26*, 2129-2135.

Vogt, A.P., Gondi, S.R., & Sumerlin, B.S. *Australian journal of chemistry* **2007**, *60*, 396-399.

Voit, B.I. & Lederer, A. *Chemical Reviews* **2009**, *109*, 5924-5973.

Wang, W.J., Wang, D., Li, B.G., & Zhu, S. *Macromolecules* **2010**, *43*, 4062-4069.

Wang, D., Zhao, T., Zhu, X., Yan, D., et al. *Chemical Society Reviews* **2015**, *44*, 4023-4071.

Williams, D. F. *Biomaterials* **2008**, *29*, 2941-2953.

Wu, D.Q., Sun, Y.X., Xu, X.D., Cheng, S.X., et al. *Biomacromolecules* **2008**, *9*, 1155.

Xiong, X.Y., Tam, K.C., & Gan, L.H. *Journal of nanoscience and nanotechnology* **2006**, *6*, 2638-2650.

Xu, J., Tao, L., Liu, J., Bulmus, V., et al. *Macromolecules* **2009**, *42*, 6893-6901.

M.A.Sc. Thesis – H. Dorrington; McMaster University – Chemical Engineering

Xu, J., Tao, L., Boyer, C., Lowe, A.B., et al. *Macromolecules* **2009**, *43*, 20-24.

Yan, D., Gao, C., & Frey, H. *Hoboken: Wiley* **2011**.

Yates, C.R. & Hayes, W. *European Polymer Journal* **2004**, *40*, 1257-1281.

Zhang, B., Ma, X., Murdoch, W., Radosz, M., et al. *Biotechnology and Bioengineering* **2013**, *110*, 990-998.

Zhang, H., Patel, A., Gaharwar, A.K., Mihaila, S.M., et al. *Biomacromolecules* **2013**, *14*, 1299-1310.

Zhao, T., Zheng, Y., Poly, J., & Wang, W. *Nature Communications* **2013**, *4*, 1873.

Zhao, C., Zhuang, X., He, P., Xiao, C., et al. *Polymer* **2009**, *50*, 4308.

Zhu, B.K., Wei, X.Z., Xiao, L., Xu, Y.Y., et al. *Polymer international* **2006**, *55*, 63-70.

**Appendix – Supplementary Information**

**Table S1.** Raw DLS data for all hyperbranched polymers.

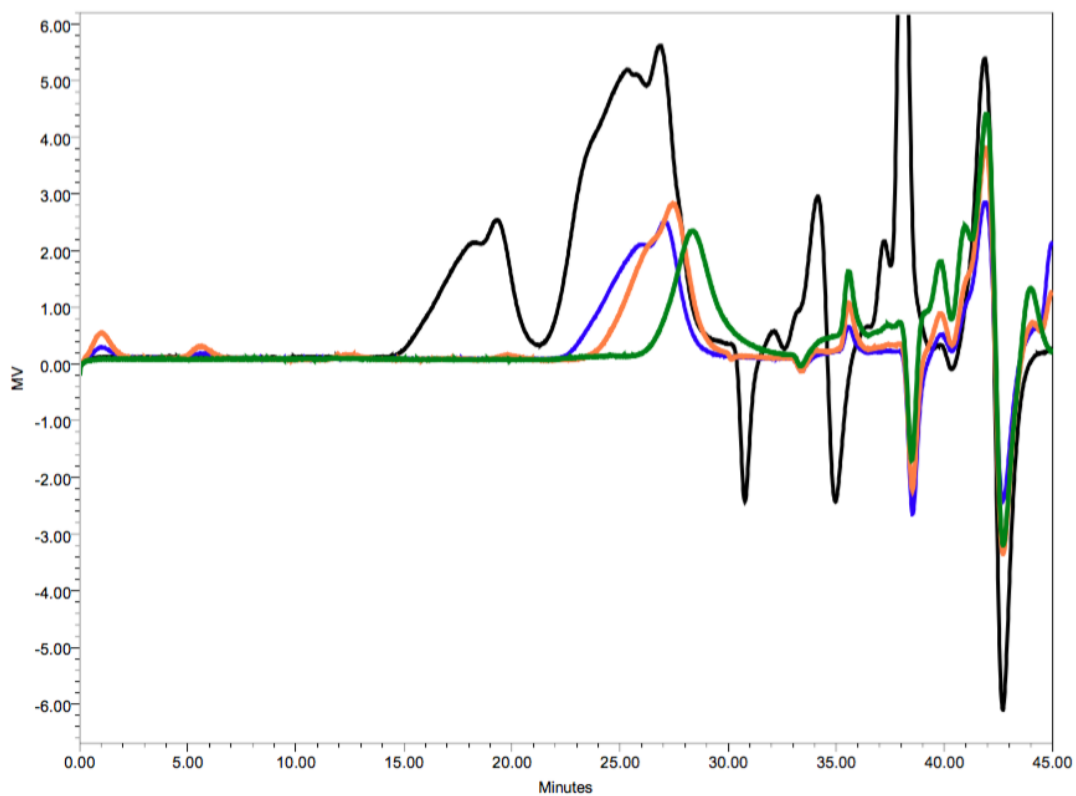


**Figure S.1.** SEC chromatogram of HBP<sub>H1522</sub> with collected samples during polymerization reaction. 2 h (green); 4 h (orange); 6 h (blue); 9 h (black).

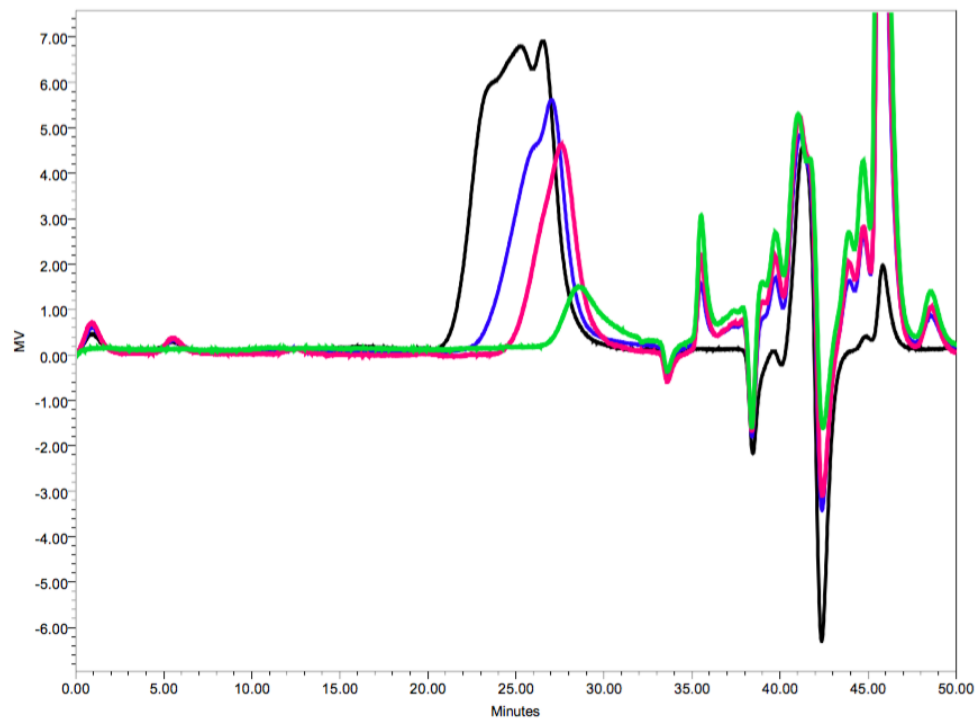


**Figure S.2.** SEC chromatogram of  $\text{HBP}_{\text{H}15_{25}}$  with collected samples during polymerization reaction. 2 h (green); 4 h (pink); 6 h (blue); 10.5 h (black).

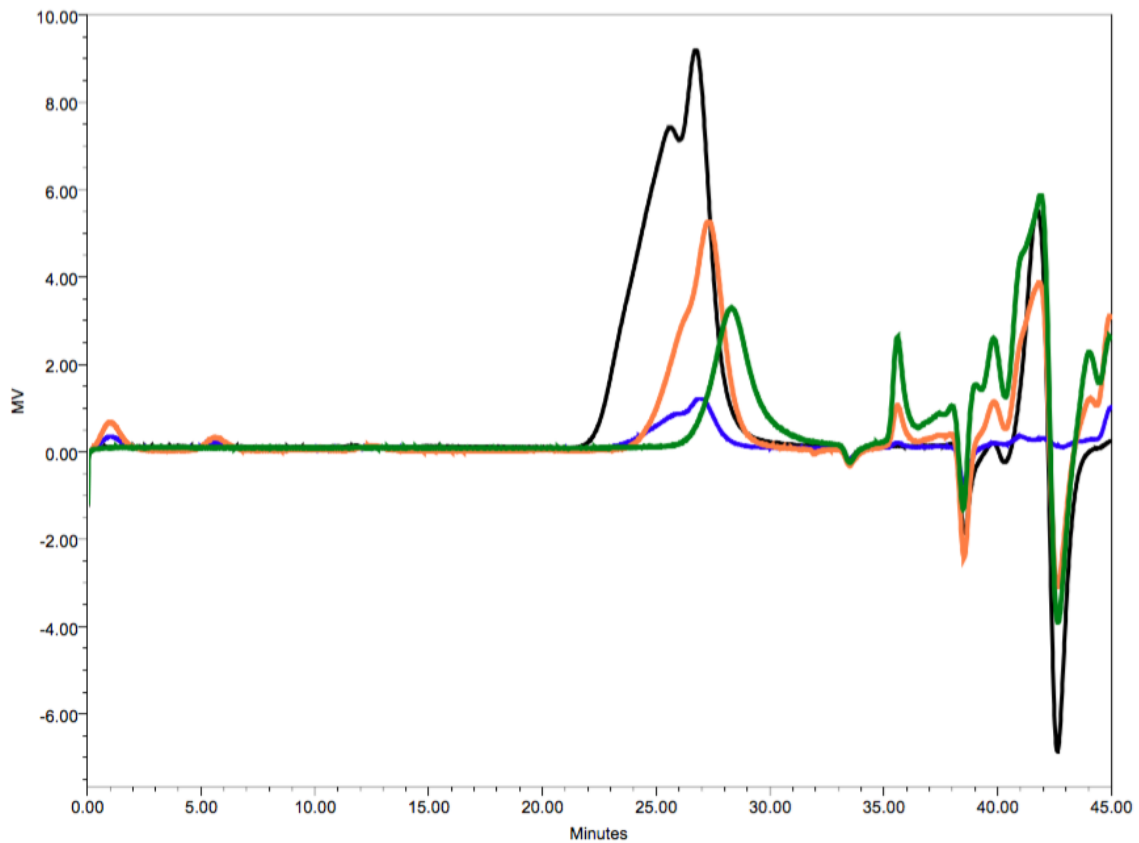


**Figure S.3.** SEC chromatogram of HBP<sub>H</sub>10 with collected samples during polymerization reaction. 2 h (green); 4 h (orange); 6 h (blue); 9 h (black).

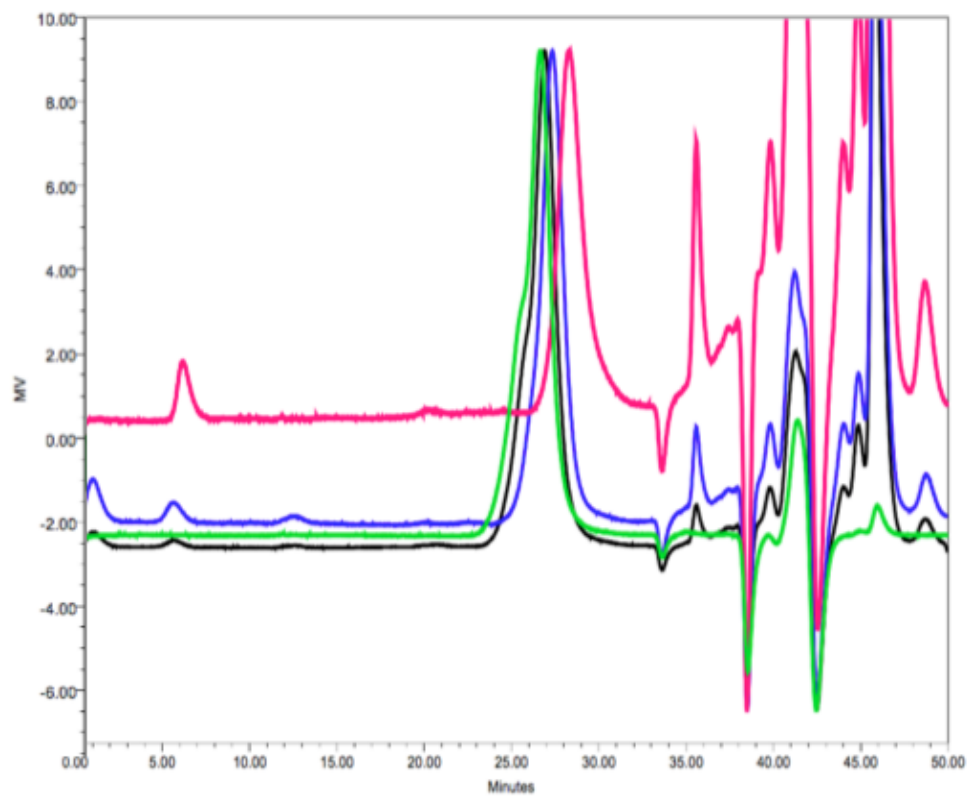


**Figure S.4.** SEC chromatogram of HBP<sub>H</sub>5 with collected samples during polymerization reaction. 2 h (pink); 4 h (blue); 6 h (black); 9 h (green).

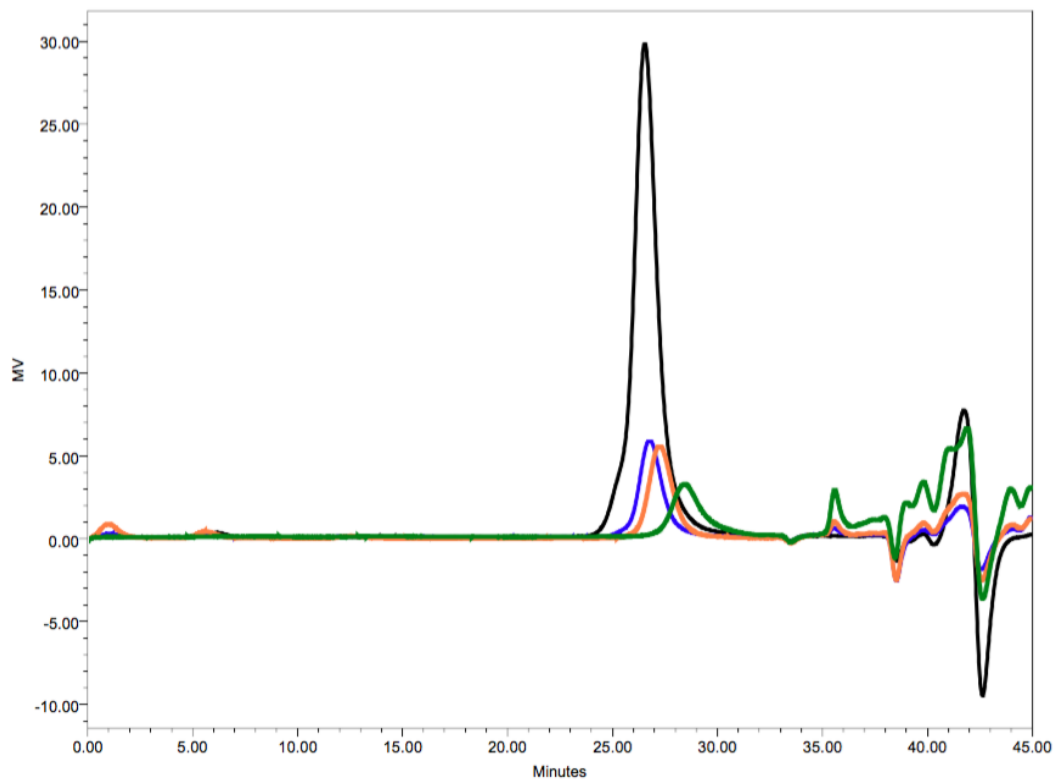


**Figure S.5.** SEC chromatogram of HBP<sub>H0</sub> with collected samples during polymerization reaction. 2 h (green); 4 h (orange); 6 h (blue); 9 h (black).

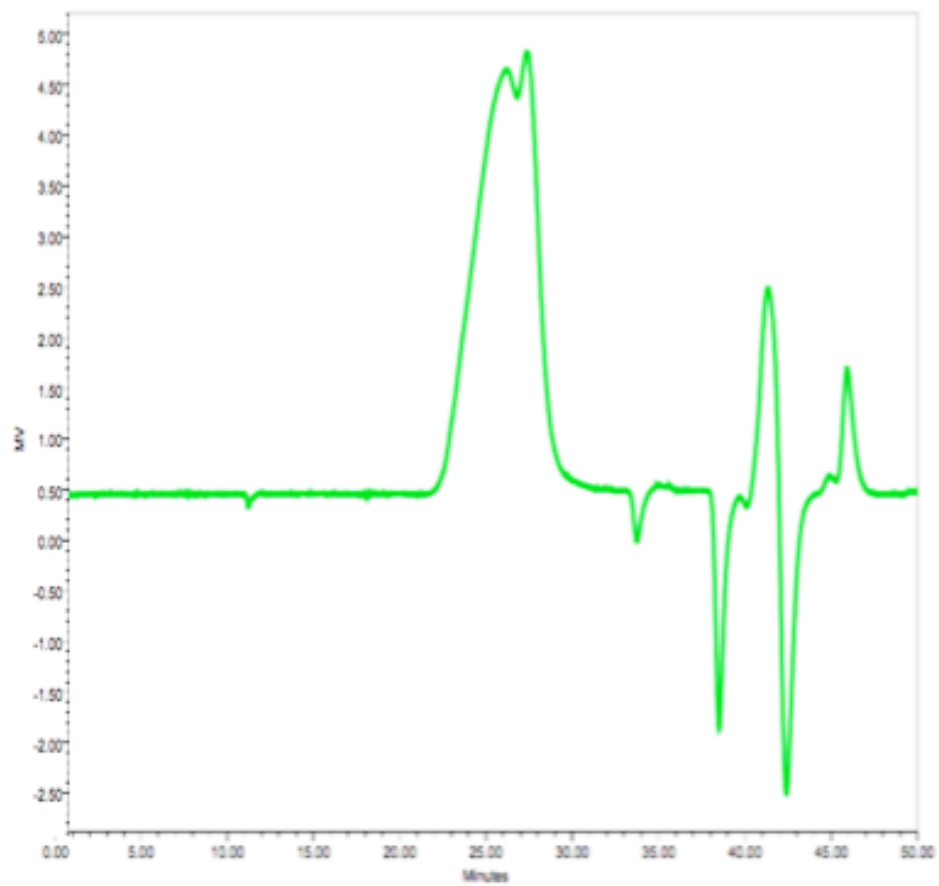


**Figure S.6.** SEC chromatogram of HBP<sub>A</sub>15 with sample taken at the end of polymerization.

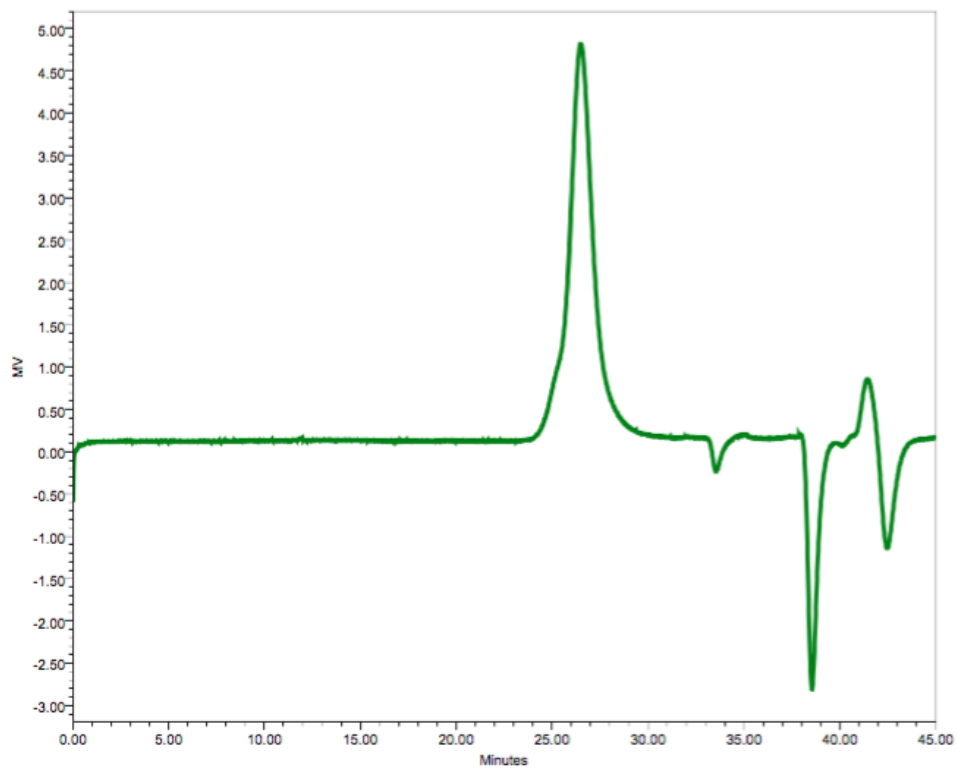


**Figure S.7.** SEC chromatogram of HBP<sub>A</sub>0 with sample taken at the end of polymerization.

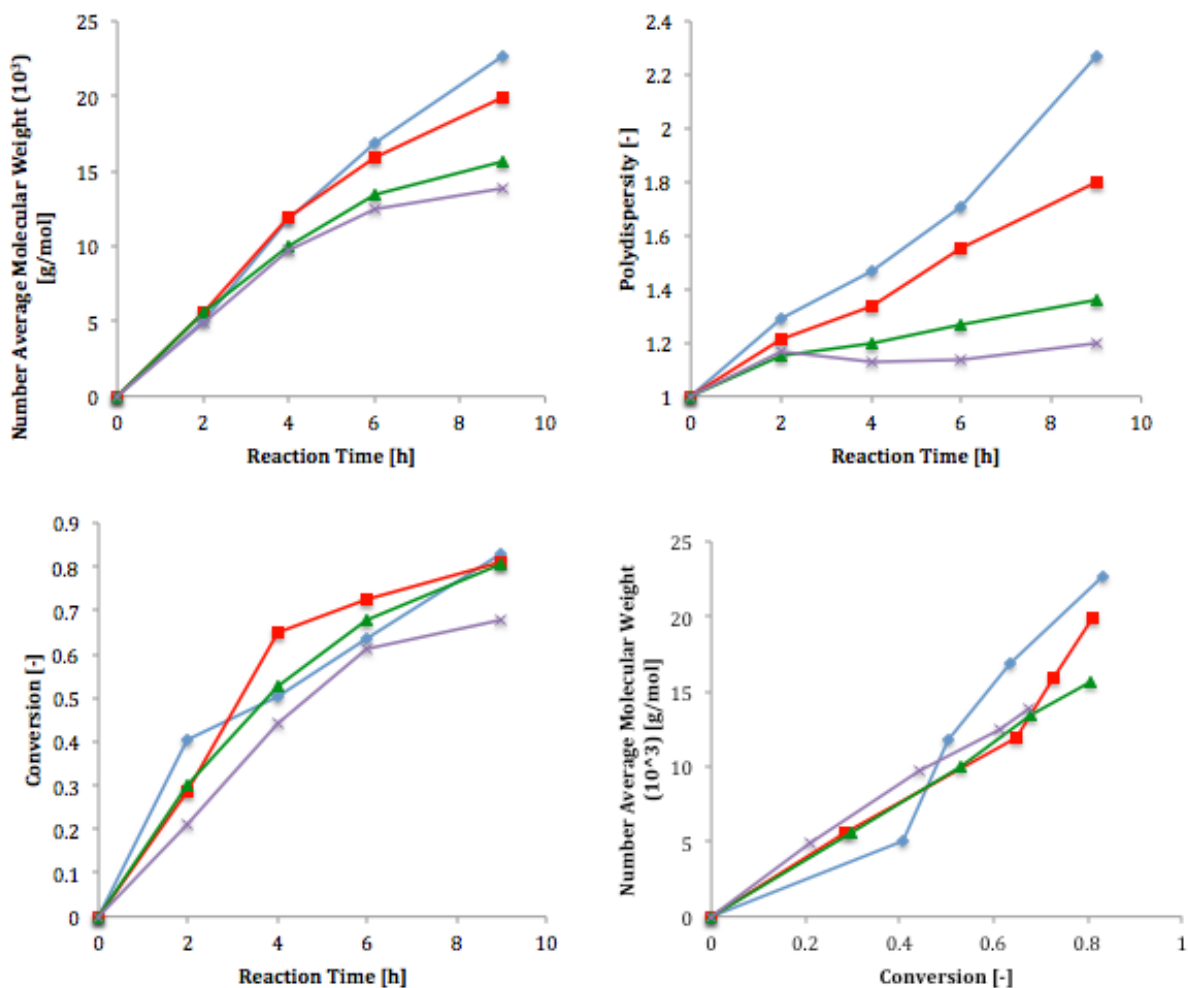


**Figure S.8.** Molecular weight, conversion, and polydispersity kinetics during the 9 hour polymerization reaction at 70°C. Samples were taken at 0, 2, 4, 6, and 9 hours. (●, blue) HBP<sub>H1522</sub>; (■, red) HBP<sub>H10</sub>; (▲, green) HBP<sub>H5</sub>; (×, purple) HBP<sub>H0</sub>.

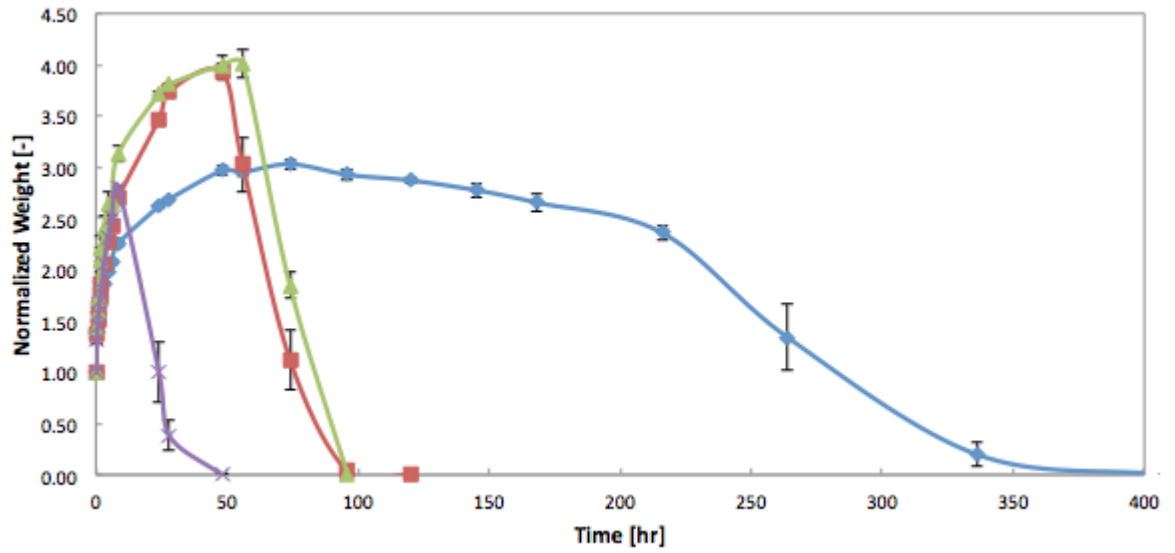


**Figure S.9.** Swelling kinetics of the varying DoB series of hyperbranched POEGMA hydrogels in 10mM PBS at 22°C. (◆, blue) HB15; (■, red) HB10; (▲, green) HB5; (×, purple) HB0. Error bars for each measurement represents one standard deviation value from the mean ( $n = 3$ ).

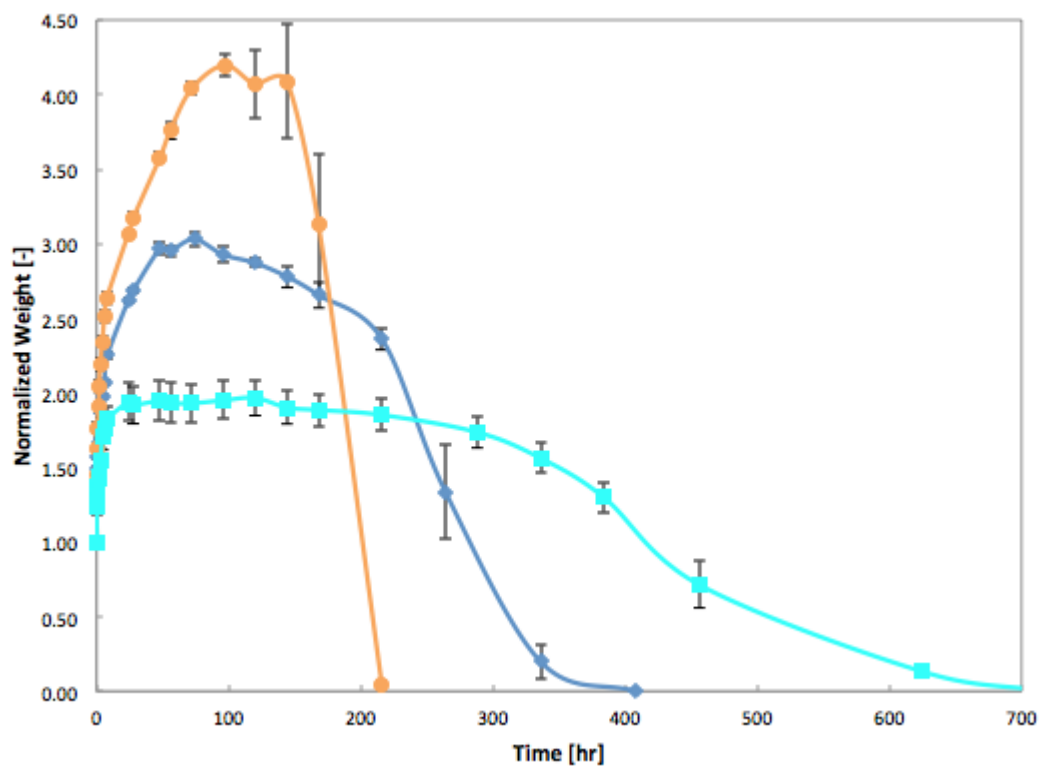


**Figure S.10.** Swelling kinetics of the 15% DoB hyperbranched POEGMA hydrogel series in 10mM PBS at 22°C. (◆, blue) HB15; (●, orange) HB15<sub>High MW</sub>; (■, aqua) HB-HB15. Error bars for each measurement represents one standard deviation value from the mean ( $n = 3$ ).